1 **Title**

2 Pan-tropical prediction of forest structure from the largest trees

3 **Authors**

4 Jean-François Bastin[1,2,3,4], Ervan Rutishauser[4,5],James R.Kellner[6,7], Sassan Saatchi[8],

5 Raphael Pélissier[9], Bruno Hérault[10,11],Ferry Slik[12], Jan Bogaert[13], Charles De Cannière[2],

6 Andrew R. Marshall[14,15,16], John Poulsen[17], Patricia Alvarez-Loyayza[18], Ana Andrade[19],

7 Albert Angbonga-Basia[20], Alejandro Araujo-Murakami[21], Luzmila Arroyo[22], Narayanan

8 Ayyappan[23,24], Celso Paulo de Azevedo[25], Olaf Banki[26], Nicolas Barbier[9], Jorcely G.

9 Barroso[26], Hans Beeckman[27], Robert Bitariho[28], Pascal Boeckx[29], Katrin Boehning-

10 Gaese[30,31], Hilandia Brandão[32], Francis Q.Brearley[33], Mireille Breuer Ndoundou Hockemba[34],

11 Roel Brienen[35], Jose Luis C.Camargo[19], Sto[36], Benoit Cassart[37,38], Jérôme Chave[39], Robin

12 Chazdon[40], Georges Chuyong[41], David B.Clark[42], Connie J.Clark[17], Richard Condit[43],

13 Euridice N. Honorio Coronado[44], Priya Davidar[22],Thalès de Haulleville[13,27], Laurent

14 Descroix[45],Jean-Louis Doucet[13],Aurelie Dourdain[46],Vincent Droissart[9],Thomas Duncan[47],

15 Javier Silva Espejo[48], Santiago Espinosa[49],Nina Farwig[50],Adeline Fayolle[13], Ted R.

16 Feldpausch[51], Antonio Ferraz[8], Christine Fletcher[36],Krisna Gajapersad[52], Jean-François

17 Gillet[13], Iêda Leão do Amaral[32], Christelle Gonmadje[53], James Grogan[54], David

18 Harris[55],Sebastian K.Herzog[56], Jürgen Homeier[57], Wannes Hubau[27], Stephen P. Hubbell[58,59],

19 Koen Hufkens[29], Johanna Hurtado[60], Narcisse.G.Kamdem[61], Elizabeth Kearsley[62], David

20 Kenfack[63], Michael Kessler[64], Nicolas Labrière[10,65], Yves Laumonier[10,66], Susan Laurance[67],

21 William F.Laurance[68], Simon L. Lewis[35], Moses B. Libalah[61], Gauthier Ligot[13], Jon Lloyd[67,68],

22 Thomas E. Lovejoy[69], Yadvinder Malhi[70], Beatriz S. Marimon[71], Ben Hur Marimon Junior[71],

23 Emmanuel H.Martin[72], Paulus Matius[73], Victoria Meyer[8], Casimero Mendoza Bautista[74], Abel

24 Monteagudo-Mendoza[75], Arafat Mtui[76], David Neill[77], Germaine Alexander Parada

25 Gutierrez[78], Guido Pardo[79],Marc Parren[80], N. Parthasarathy[23],Oliver L. Phillips[35], Nigel C.A.

26 Pitman[80], Pierre Ploton[9],Quentin Ponette[37], B.R.Ramesh[23], Jean-Claude

27 Razafimahaimodison[81],Maxime Réjou-Méchain[9], Samir Gonçalves Rolim[82], Hugo Romero

28 Saltos[83], Luiz Marcelo Brum Rossi[82], Wilson Roberto Spironello[32], Francesco Rovero[76],

29 Philippe Saner[84], Denise Sasaki[85], Mark Schulze[86], Marcos Silveira[87], James Singh[88], Plinio

30 Sist[10,89], Bonaventure Sonke[61],J.Daniel Soto[90], Cintia Rodrigues de Souza[24], Juliana

31 Stropp[91], Martin J.P. Sullivan[35], Ben Swanepoel[34], Hans ter Steege[25,92],John

32 Terborgh[93,94],Nicolas Texier[95], T.Toma[96], Renato Valencia[97], Luis Valenzuela[75], Leandro

33 Valle Ferreira[98], Fernando Cornejo Valverde[99], Tinde R Van Andel[25],Rodolfo Vasque[77], Hans

34 Verbeeck[62],Pandi Vivek[22],Jason Vleminckx[100], Vincent A.Vos[79,101], Fabien H.Wagner[102],

35 Warsudi[103],Verginia Wortel[104], Roderick J. Zagt[105],Donatien Zebaze[61]

36 1. Institute of Integrative Biology, Department of Environmental Systems Science, ETH

37 Zürich, 8092 Zürich, Switzerland

38 2. Landscape Ecology and Plant Production System, Université libre de Bruxelles.

39 CP264-2, B-1050 Bruxelles, Belgium

40 3. Affiliated during analysis and writing at NASA, Jet Propulsion Laboratory, California

41 Institute of Technology, 4800 Oak Grove Drive, Pasadena, CA 91109, USA

42 4. Carboforexpert (carboforexpert.ch), 1248 Hermance, Switzerland

43 5. Smithsonian Tropical Research Institute, Box 0843-03092, Balboa, Ancon, Panama

44 6. Department of Ecology and Evolutionary Biology, Brown University, Providence, RI

45 02912, USA

46 7. Institute at Brown for Environment and Society, Brown University, Providence, RI

47 02912, USA

48 8. NASA, Jet Propulsion Laboratory, California Institute of Technology, 4800 Oak Grove

49 Drive, Pasadena, CA 91109, USA

50 9. AMAP Lab, IRD, CIRAD, CNRS, INRA, Univ. Montpellier, Montpellier, France

51 10. Cirad, UR Forest & Societies, 34398 Montpellier Cedex 5, France

52   11.   INPHB (Institut National Polytechnique Félix Houphouet Boigny), Yamoussoukro,

53   Ivory Coast

54   12.   Faculty of Science, Universiti Brunei Darusallam, Gadong, Brunei Darussalam

55   13.   Gembloux Agro-Bio Tech, Université de Liège, B-5030 Gembloux, Belgium

56   14.   CIRCLE, Environment Department, Wentworth Way, University of York, Heslington,

57   York, YO10 5NG, UK

58   15.   Tropical Forests and People Research Centre, University of the Sunshine Coast, QLD

59   4556, Australia

60   16.   Flamingo Land Ltd., Kirby Misperton, YO17 6UX, UK

61   17.   Nicholas School of the Environment, Duke University, PO Box 90328, Durham, NC

62   27708, USA

63   18.   Field Museum of Natural History, Chicago, USA.

64   19.   Biological Dynamics of Forest Fragment Project (BDFFP - INPA/STRI), Manaus -

65   Amazonas, Brazil

66   20.   Institut Facultaire des Sciences Agronomiques de Yangambi. DRC

67   21.   Museo de Historia Natural Noel Kempff Mercado, Santa Cruz, Bolivia

68   22.   Department of Ecology and Environmental Sciences, Pondicherry University, Kalapet,

69   Pondicherry 605014, India

70   23.   French Institute of Pondicherry (IFP), 11 Saint Louis Street, Pondicherry 605 001,

71   India

72   24.   Embrapa Amazônia Ocidental, Brazil

73   25.   Naturalis Biodiversity Centre, PO Box 9517, 2300 RA Leiden, The Netherlands

74   26.   Universidade Federal do Acre, Campus Floresta, Cruzeiro do Sul, Acre, Brazil

75   27.   Service of Wood Biology, Royal Museum for Central Africa, Tervuren, Belgium

76   28.   Institute of Tropical Forest Conservation, Mbarara University of Science and

77   Technology, Uganda.

78   29.   Isotope Bioscience Laboratory – ISOFYS, Ghent University, Belgium

79   30.   Senckenberg Biodiversity and Climate Research Centre (BiK-F), Frankfurt am Main,

80   Germany

81   31.   Dept of Biological Sciences, Goethe Universität, Frankfurt am Main, Germany

82   32.   National Institute for Amazonian Research (INPA), Manaus, Amazonas, Brazil

83   33.   School of Science and the Environment, Manchester Metropolitan University, Chester

84   Street, Manchester, M1 5GD, UK

85   34.   Wildlife Conservation Society, New York, USA

86   35.   School of Geography, University of Leeds, Leeds, UK

87   36.   Malaysia Campus, Jalan Broga, Semenyih 43500, Selangor, Malaysia

88   37.   UCL-ELI, Earth and Life Institute, Université catholique de Louvain, Louvain-la-Neuve

89   BE-1348, Belgium

90   38.   Ecole Régionale Post-universitaire d'Aménagement et de Gestion Intégrés des Forêts

91   et Territoires Tropicaux, Kinshasa, DRC

92   39.   Laboratoire Evolution et Diversité biologique, CNRS & Université Paul Sabatier,

93   Toulouse 31062, France

94   40.   Department of Ecology and Evolutionary Biology, University of Connecticut, Storrs,

95   Connecticut 06268-3043, USA

96   41.   Department of Botany and Plant Physiology, University of Buea, Cameroon

97   42.   Department of Biology, University of Missouri-St Louis, Missouri, USA

98 43. Field Museum of Natural History and Morton Arboretum, Illinois, USA

99 44. Coronado, Inst. de Investigaciones de la Amazonia Peruana, Iquitos, Peru

100 45. ONF pôle R&D, Cayenne, France

101 46. Cirad, UMR EcoFoG (AgroParisTech, CNRS, Inra, Universite des Antilles, Universite

102 de la Guyane), Kourou, French Guiana

103 47. Department of Botany and Plant Pathology, Oregon State University, Corvallis, OR

104 97331, USA

105 48. Departamento de Biología, Universidad de La Serena, Casilla 554 La Serena, Chile

106 49. Universidad Autónoma de San Luis Potosí, San Luis Potosí, México

107 50. Department of Conservation Ecology, Philipps-Universität Marburg, Karl-von-Frisch-

108 Straße 8, 35032 Marburg, Germany

109 51. Geography, College of Life and Environmental Sciences, University of Exeter, Exeter,

110 EX4 4RJ, UK

111 52. Conservation International Suriname, Paramaribo, Suriname

112 53. Department of Plant Biology, Faculty of science, University of Yaounde I, BP 812

113 Yaoundé, Cameroon

114 54. Mount Holyoke College Botanic Garden, South Hadley, MA 01075, USA

115 55. Royal Botanic Garden Edinburgh, Edinburgh EH3 5LR, UK

116 56. Museo de Historia Natural Alcide d'Orbigny, Cochabamba, Bolivia

117 57. Plant Ecology, University of Goettingen, Untere Karspuele 2, 37073 Goettingen,

118 Germany

119 58. Department of Ecology and Evolutionary Biology, University of California, Los

120 Angeles, California 90095, USA

59. Smithsonian Tropical Research Institute, Apartado 0843-03092, Balboa, Republic of Panama

60. Organization for Tropical Studies, Costa Rica

61. Plant Systematic and Ecology Laboratory, Higher Teacher's Training College, University of Yaoundé I, P.O. Box 047, Yaoundé, Cameroon.

62. CAVElab – Computational and Applied Vegetation Ecology, Ghent University, Belgium

63. CTFS-ForestGEO, Smithsonian Tropical Research Institute, MRC 166, NMNH, P.O. Box 37012, Washington, DC 20013-7012, USA

64. Department of Systematic and Evolutionary Botany, University of Zurich, Zollikerstrasse 107, Zurich 8008, Switzerland

65. AgroParisTech, Doctoral School ABIES, 19 Avenue du Maine, 75732 Paris Cedex 15, France

66. Center for International Forestry Research, Jl. CIFOR, Situ Gede, Bogor Barat 16115, Indonesia

67. Centre for Tropical Environmental and Sustainability Science, College of Science and Engineering, James Cook University, Cairns, Queensland 4870, Australia.

68. Department of Life Sciences, Imperial College London, SL5 7PY, Ascot, UK

69. Department of Environmental Science and Policy, George Mason University, Fairfax, VA, USA

70. Environmental Change Institute, School of Geography and the Environment, University of Oxford, Oxford, UK

71. Universidade do Estado de Mato Grosso, Campus de Nova Xavantina, Nova Xavantina, MT, Brazil

145   72.   Udzungwa Ecological Monitoring Centre, Udzungwa Mountains National Park,

146   Tanzania, Sokoine University of Agriculture, Morogoro, Tanzania

147   73.   Escuela de Ciencias Forestales, Unidad Académica del Trópico, Universidad Mayor

148   de San Simón, Sacta, Bolivia

149   74.   Faculty of Forestry, Mulawarman University, Indonesia

150   75.   Jardín Botánico de Missouri, Oxapampa, Pasco, Peru.

151   76.   MUSE - Museo delle Scienze, Trento, Italy

152   77.   Universidad Estatal Amazónica, Puyo, Pastaza, Ecuador

153   78.   Museo de Historia Natural Noel Kempff Mercado, Santa Cruz, Bolivia

154   79.   Universidad Autónoma del Beni, Riberalta, Bolivia

155   80.   Science and Education, The Field Museum, 1400 South Lake Shore Drive, Chicago,

156   Illinois 60605–2496, USA

157   81.   Centre ValBio, Ranomafana, Madagascar

158   82.   Embrapa Florestas, Colombo/PR, Brazil

159   83.   Yachay Tech University, School of Biological Sciences and Engineering. Urcuquí,

160   Ecuador

161   84.   Department of Evolutionary Biology and Environmental Studies, University of Zurich,

162   CH-8057 Zurich, Switzerland

163   85.   Fundação Ecológica Cristalino Alta Floresta, Brazil

164   86.   HJ Andrews Experimental Forest, PO Box 300, Blue River, OR 97413, USA

165   87.   Museu Universitário, Universidade Federal do Acre, Rio Branco 69910-900, Brazil

166   88.   Guyana Forestry Commission, Georgetown, Guiana

167   89.   Forests and Societies, Univ. Montpellier, CIRAD, Montpellier, France

168   90.   Museo de Historia Natural Noel Kempff Mercado, Santa Cruz, Bolivia

169   91.   Institute of Biological and Health Sciences, Federal University of Alagoas, Maceió,

170   Brazil

171   92.   Systems Ecology, Free University, De Boelelaan 1087, Amsterdam, 1081 HV,

172   Netherlands.

173   93.   Florida Museum of Natural History and Department of Biology, University of Florida -

174   Gainesville, Gainesville, FL 32611, USA

175   94.   Department of Biology, James Cook University, Cairns, Australia

176   95.   Laboratoire d'Evolution Biologique et Ecologie, Faculté des Sciences, Université libre

177   de Bruxelles, CP160/12, 1050 Bruxelles, Belgium

178   96.   Forestry and Forest Products Research Institute, Matsunosato 1, Tsukuba 305-8687,

179   Japan

180   97.   Escuela de Ciencias Biológicas, Pontificia Universidad Católica del Ecuador, Quito,

181   Ecuador

182   98.   Coordenação de Botânica, Museu Paraense Emilio Goeldi, Belém, Brazil

183   99.   Andes to Amazon Biodiversity Program, Madre de Dios, Peru

184   100. Department of Integrative Biology, University of California, Berkeley, 1005 Valley Life

185   Sciences Building 3140, Berkeley, CA 94720-3140, USA

186   101. Centro de Investigación y Promoción del Campesinado - Norte Amazónico, Riberalta,

187   Bolivia

188   102. Remote Sensing Division, National Institute for Space Research - INPE, São José

189   dos Campos 12227-010, SP, Brazil

190   103.   The Center for Reforestation Studies in the Tropical Rain Forest (PUSREHUT),

191   Mulawarman University, Jln. Kihajar Dewantara Kampus Gunung Kelua, Samarinda 75123,

192   East Kalimantan, Indonesia

193   104.   Center for Agricultural Research in Suriname (CELOS), Suriname

194   105.   Tropenbos International, PO Box 232, Wageningen 6700 AE, The Netherlands

Abstract

Aim. Large tropical trees form the interface between ground and airborne observations, offering a unique opportunity to capture forest properties remotely. However, despite rapid development of metrics to characterize the forest canopy from remotely sensed data, a gap remains between aerial and field inventories. To close this gap, we propose a new pan-tropical model to predict plot-level forest structure properties and biomass from just the largest trees, as a proxy for the whole plot inventory.

Location. Pan-tropical

Method. Using a dataset of 867 plots distributed among 118 sites across the tropics, we tested the ability to predict quadratic mean diameter, basal area, Lorey's height and community wood density from the ith largest trees, i.e. testing the cumulative information gathered from these i trees ranked by decreasing diameter. These tests served as a basis to select the optimal number of the largest trees and further predict plot-level biomass from a single model.

Result. Focusing on readily available information captured by airborne remote sensing, we show that measuring the largest trees in tropical forests enables unbiased predictions of plot and site-level forest structure. The 20 largest trees per hectare predicted quadratic mean diameter, basal area, Lorey's height and community wood density with 12%, 16%, 4% and 4% of relative error. Building on this result, we developed a new model to predict plot-level AGB from measurements of the 20 largest trees. This model allows an independent and unbiased prediction of biomass with 17.7% of error compared to ground estimates. Most of the remaining error is driven by differences in the proportion of total biomass held in medium size trees (50-70 cm), which shows some continental dependency with American tropical forests presenting the highest levels of total biomass share in these intermediate diameter classes.

Conclusion. Our approach provide new information on tropical forest structure and can be employed to generate accurately field estimates of tropical forest carbon stocks to support the calibration and validation of current and forthcoming space missions. It will reduce the cost of programs to monitor, report, and verify forest resources, and will contribute to scientific understanding of tropical forest ecosystems and response to climate change.

Introduction

The fundamental ecological function of large trees is well established for tropical forests. They offer shelter to a multiple organisms (Remm & Lõhmus, 2011; Lindenmayer *et al.*, 2012), regulate forest dynamics, regeneration (Harms *et al.*, 2000; Rutishauser *et al.*, 2010) and total biomass (Stegen *et al.*, 2011), and are important contributor to the global carbon cycle (Meakem *et al.*, 2017). Being major components of the canopy, the largest trees also suffer more than sub-canopy and understory trees from climate change, as they are directly exposed to variations in solar radiation, wind strength, temperature seasonality and relative air humidity (Laurance *et al.*, 2000; Nepstad *et al.*, 2007; Lindenmayer *et al.*, 2012; Thomas *et al.*, 2013; Bennett *et al.*, 2015; Meakem *et al.*, 2017). Because they are visible from the sky, large trees are ideal for monitoring forest responses to climate change via remote sensing (Bennett *et al.*, 2015; Asner *et al.*, 2017).

Large trees encompass a disproportionate fraction of total above-ground biomass (AGB) in tropical forests (Chave *et al.*, 2001), with some variations in their relative contribution to the total AGB among the tropical regions (Feldpausch *et al.*, 2012). In Central Africa, the largest 5% of trees, i.e. the 5% of trees with the largest diameter at 130 cm per area, store 50% of forest aboveground biomass on average (Bastin *et al.*, 2015). Consequently, the density of large trees largely explains variation in AGB at local (Clark & Clark, 1996), regional (Malhi *et al.*, 2006; Saatchi *et al.*, 2007), and continental scales (Stegen *et al.*, 2011; Slik *et al.*, 2013). Detailing the contribution of each single tree to the diameter structure, we showed previously that plot-level AGB can be predicted from a few large trees (Bastin *et al.*, 2015), with the measurement of the 20 largest trees per hectare being sufficient to estimate plot-level biomass with less than 15% errors in reference to ground estimates. These findings opened the possibility of measuring the largest trees to cost-effectively monitor forest biomass in Central Africa, rather than conducting full inventories of all size classes. Similarly, they suggested that remote sensing (RS) approaches should focus on the measurement of the largest trees, instead of properties of the entire forest.

250   Several efforts are underway to close the gap between remote sensing and field surveys (e.g.

251   Jucker et al. 2016a, Coomes et al. 2017). However, field inventories still rely on exhaustive

252   data collection, while remote sensing surveys provide a limited alternative for the following

253   reasons. Existing RS approaches that provide predictions of biomass with less than 20% error

254   for 1 ha plot size are either specific to the relationship between forest type and image/scene

255   properties (Barbier *et al.*, 2011; Asner *et al.*, 2012; Barbier & Couteron, 2015), or require

256   ground measurement of all trees above or equal to 10 cm of D for calibration (Asner *et al.*,

257   2012; Asner & Mascaro, 2014). Using mean canopy height extracted from active sensors

258   (Mascaro *et al.*, 2011; Ho Tong Minh *et al.*, 2016), or canopy grain derived from optical images

259   (Proisy *et al.*, 2007; Ploton *et al.*, 2012, 2017; Bastin *et al.*, 2014), the biomass is predicted

260   from remote sensing with a typical error of only 10-20% compared to ground-based estimates,

261   but is limited to the extent of the scene used. An interesting development to alleviate this spatial

262   restriction lies in the 'universal approach', proposed by Asner et al. (2012) and further adapted

263   in Asner and Mascaro (2014), in which plot-level biomass is predicted by a linear combination

264   of ground-based and remotely-sensed metrics. The 'universal approach' relies upon canopy

265   height metrics derived from radar or LiDAR (top of canopy height, TCH), and basal area (BA,

266   i.e. the cross-sectional stem area) and community wood density (i.e. weighted by basal area,

267   WD_{BA}) derived from full field inventories. AGB is then predicted as follows (Asner *et al.*, 2012):

268    $AGB = aTCH^{b1}BA^{b2}WD_{BA}^{b3}$ (1)

269   While generally performing better than approaches based solely on remote sensing of tree

270   height (Coomes *et al.*, 2017), this model largely relies on exhaustive ground measurements

271   (i.e. wood density and basal area of all trees above 10 cm of diameter at 130 cm, neither of

272   which is measured using any existing remotely sensed data).

273   Recent advances in remote sensing allow the identification of single trees in the canopy (Ferraz

274   *et al.*, 2016), estimation of adult mortality rates for canopy tree species (Kellner & Hubbell,

275   2017), description of the forest diameter structure (Stark *et al.*, 2015), depiction of crown and

276   gap shapes (Coomes *et al.*, 2017), and even identification of some functional traits of canopy

277   species (Asner *et al.*, 2017). Building upon this work, we test the capacity of metrics from the

278   largest trees that can be potentially derived using remote sensing to predict plot-level biomass

279   (i.e. the summed AGB of all live trees D ≥10 cm in a plot). To this end, we tested the following

280   model:

281   $AGB = a(Dg_{LT\,i} H_{LT\,i} WD_{LT\,i})^{b1}$ (2)

282   Where for the ith largest trees, Dg_{LT} is the quadratic mean diameter, H_{LT} the mean height, and

283   WD_{LT} the mean wood density averaged among the ith largest trees.

284   Using a large database of forest inventories gathered across the Tropics (Figure 1), including

285   secondary and old growth forest plots, we test the ability of the largest trees to provide

286   information on various metrics estimated at 1-ha plot level, such as the mean quadratic

287   diameter, the basal area (BA), the Lorey's height (i.e. plot-average height weighted by BA), the

288   community wood density (i.e. plot-average wood density weighted by BA) and mean above-

289   ground live biomass (AGB) (supplementary figure 1). While previous work focused on

290   estimating biomass in Central African forests (Bastin *et al.*, 2015), the present study aims at

291   generalizing the potential of large trees in predicting these different plot metrics at continental

292   and pan-tropical scales. Taking advantage of a unique dataset gathered across the tropics (XX

293   ha, YYY plots), we also investigate major differences in forest structure across the three main

294   tropical regions, South America, Africa and South East Asia. We further discuss how this

295   approach can be used to guide innovative RS techniques and increase the frequency and

296   representativeness of ground data to support global calibration and validation of current and

297   planned space missions. These include the NASA Global Ecosystem Dynamics Investigation

298   (GEDI), NASA-ISRO Synthetic Aperture Radar (NISAR), and ESA P-band radar (BIOMASS).

299   This study is a step forward in bringing together remote sensing and field sampling techniques

300   for quantification of terrestrial C stocks in tropical forests.

Material & Methods

Database

For this study, we compiled standard forest inventories conducted in 867 1-hectare plots from 118 sites across the three tropical regions (Figure 1), including mature and secondary forests. Each site comprises all the plots in a given geographical location, i.e. within a 10 km radius and collected by a PI and its team. These consisted of 389 plots in America (69 sites), 302 plots in Africa (35 sites) and 176 plots in Asia (14 sites). Data were provided by Principal Investigators (see supplementary Table 1), and through datasets available at ForestPlots (https://www.forestplots.net/), TEAM (http://www.teamnetwork.org/) and CTFS (http://www.forestgeo.si.edu/) networks.

We selected plots located between 23°N and 23°S, including tropical islands, with an area of at least 1-ha to ensure stable intra-sample variance in basal area (Clark & Clark, 2000). Plots in which at least 90% of the stems were identified to species, and in which all stems with the diameter at 130 cm greater than or equal to 10 cm had been measured were included. Wood density, here recorded as the wood dry mass divided by its green volume, was assigned to each tree using the lowest available taxonomic level of botanical identifications (i.e. species or genus) and the corresponding average wood density recorded in the Global Wood Density Database (GWDD, Chave *et al.*, 2009; Zanne *et al.*, 2009). Botanical identification was harmonized through the Taxonomic Names Resolution Service (http://tnrs.iplantcollaborative.org), for both plot inventories and the GWDD. For trees not identified to species or genus (~5%), we used plot-average wood density. We estimated heights of all trees using Chave et al.'s (2014) pan-tropical diameter-height model which accounts for heterogeneity in the D-H relationship using an environmental proxy:

$Ln(H) = 0.893 - E + 0.760 ln(D) - 0.0340 ln(D)^2$ (3)

Where D is the diameter at 130cm and E is a measure of environmental stress (Chave *et al.*, 2014). For sites with tree height measurements (N=20), we developed local D-H models, using a Michaelis-Menten function (Molto *et al.*, 2014). We used these local models to validate the

328   predicted Lorey's height (i.e. plot average height weighted by BA) from the largest trees, of

329   which height has been estimated with a generic H-D model (equation 3, Chave et al. 2014).

330   We estimated plot biomass as the sum of the biomass of live tree with diameter at 130 cm

331   superior or equal to 10 cm, using the following pan-tropical allometric model (Réjou-Méchain

332   *et al.*, 2017):

333     $AGB = \exp(-2.024 - 0.896E + 0.920\ln(WD) + 2.795\ln(D) - 0.0461(\ln(D^2)))$ (4)

334   **Plot-level metric estimation from the largest trees**

335   The relationship between each plot metric, namely basal area (BA), the quadratic mean

336   diameter (Dg), Lorey's height (H_{BA}; the mean height weighted by the basal area) and the

337   community wood density (WD_{BA}; the mean wood density weighted by the basal area), and

338   those derived from largest trees was determined using an iterative procedure following Bastin

339   et al. (2015). Trees were first ranked by decreasing diameter in each plot. An incremental

340   procedure (i.e. including a new tree at each step) was used to sum or average information of

341   the *i* largest trees for each plot metric. Specifically, each plot-level metric was predicted by the

342   respective metric derived from the ith largest trees. For each increment, the ability (goodness

343   of fit) of the *i* largest trees to predict a given plot-metric was tested through a linear regression.

344   To avoid overfitting, a Leave-One-Out procedure was used to develop independent site-

345   specific models (N=118). Specifically, the model to be tested at a site was developed with data

346   from all other sites. Errors were then estimated as the relative root mean square error (rRMSE)

347   computed between observed and predicted values (X):

348     $rRMSE = \bar{X} \sum \sqrt{\dfrac{(Xobs - Xpred)^2}{n}}$ (5)

349   The form of the regression model (i.e. linear, exponential) was selected to ensure a normal

350   distribution of the residuals.

351   To estimate plot basal area, we used a simple power-law constrained on the origin, as linear

352   model resulted in non-normal residuals. Plot-level basal area (BA) was related to the basal

353   area for the *i* largest trees (BA_i) using:

354     $BA = b_1 \sum BA_i^{\gamma 1}$ (6)

355 To estimate the quadratic mean diameter, Lorey's height and the wood density of the

356 community, we used simple linear models relating the plot-level metrics and the value of the

357 metrics for the *i* largest trees:

358 $D_g = a_2 + b_2 D_{gi}$ (7)

359 $H_{BA} = a_3 + b_3 \overline{H_i}$ (8)

360 $WD_{BA} = a_4 + b_4 \overline{WD_i}$ (9)

361 Both Lorey's height (H_{BA}) and the average height ($\overline{H_i}$) of the ith largest trees depend on the

362 same D-H allometry, which always contains uncertainty whether we use a local, a continental

363 or a pan-tropical model. To test the dependence of the prediction of H_{BA} from $\overline{H_i}$ on the

364 allometric model, we used measurement from Malebo in the Democratic Republic of the

365 Congo, where all heights were measured on the ground (see supplementary figure 2).

366 The quality of the predictions of plot-level metrics from the largest trees is quantified using the

367 relative root mean square error (rRMSE) between measured and predicted values, and

368 displayed along the cumulated number of largest trees (Figure 2). Model coefficients are

369 estimated for each metric derived from the largest trees (N_{LT}) and averaged across the 118

370 models (see supplementary table 2).

371 Mean rRMSE is plotted as a continuous variable, while its variation is presented as a

372 continuous area between 5th and the 95th percentiles of observed rRMSE (Figure 2).

373 **The optimal number of largest trees for plot-level biomass estimation**

374 The optimal number of largest trees N_{LT} was determined from the prediction of each plot-level

375 metric considered above, i.e. keeping a small number of trees while ensuring a low level of

376 error for each structural parameter. We then predicted plot-level biomass from the N_{LT} model

377 (equation 2). The final error was calculated by propagating the entire set of errors related to

378 equation 4 (Réjou-Méchain *et al.*, 2017) in the N_{LT} model (i.e. error associated to each allometric

379 model used). The model was then cross-validated across all plots (N=867).

380 **Investigating residuals: what the largest trees do not explain**

381 To understand the limits of predicting AGB through N_{LT}, we further investigated the relationship

382 between AGB residuals and key structural and environmental variables using linear modelling.

383 Forest structure was investigated through the total stem density (N), the quadratic mean

384 diameter (Dg), Lorey's height (H_{BA}) and community wood density (WB_{BA}). As environmental

385 data, we used the mean annual rainfall and the mean temperature computed over the last 10

386 years at each site using the Climate Research Unit data (New *et al.*, 1999, 2002), along with

387 rough information on soil types (Carré. *et al.*, 2010). Major soil types were computed from the

388 soil classification of the Harmonized World Soil Database into IPCC (intergovernmental panel

389 on climate change) soil classes. In addition, considering observed differences in forest

390 structure across tropical continents (Feldpausch *et al.*, 2011) and recent results on pan-tropical

391 floristic affinities (Slik *et al.*, 2015), we tested for an effect of continent (America, Africa and

392 Asia) on the AGB residuals.

393 The importance of each variable was evaluated by calculating the type II sum of squares that

394 measures the decrease in residual sum of squares due to an added variable once all the other

395 variables have been introduced into the model (Langsrud, 2003). Residuals were investigated

396 at both plot and site levels, the latter analyzed to test for any influence of the diameter structure,

397 which is usually unstable at the plot level due to the dominance of large trees on forest metrics

398 at small scales (Clark & Clark, 2000). Here we use a principal component analysis (PCA) to

399 summarize the information held in the diameter structure by ordinating the sites along the

400 abundance of trees in each diameter class (from 10 to +100 cm by 10 cm bins).

401

Results

Plot-level metrics

Plot metrics averaged at the site level (867 plots, 118 sites) present important variations within and between continents. In our database, the quadratic mean diameter varies from 15 to 42 cm^2ha^{-1}, the basal area from 2 to 58 m^2ha-1, Lorey's height from 11 to 33 m and the wood density weighted by the basal area from 0.48 to 0.84 gcm^{-3} (Supplementary figure 1). Such important differences between minimal and maximal values are observed because our database cover sites with various forest types, from young forest colonizing savannas to old growth forest. However, most of our sites are found in mature forests, as shown by relatively high average and median value of each plot metric (average aboveground biomass = 302 $Mgha^{-1}$; supplementary figure 1). In general, highest values of aboveground biomass are found in Africa, driven by highest values of basal area and highest estimations of Lorey's height. Highest values of wood density weighted by basal area are found in America.

Plot-level estimation from the i largest trees

Overall, plot metrics at 1 ha scale were well predicted by the largest trees, with qualitative agreement among global and continental models (Figure 2).

When using the 20 largest trees to predict basal area (BA) and quadratic mean diameter (Dg), the mean rRMSE was < 16% and 12%, respectively (Figs 3a and 3b). Lorey's height (H_{BA}) and wood density weighted by basal area (WD_{BA}) were even better predicted (Figs 3c and 3d), with mean rRMSE of 4% for the 20 largest trees. The prediction of Lorey's height from the largest trees using local diameter-height model (supplementary Figure 2a) yielded results similar to those obtained using equation 3 of Chave et al. (2014). More importantly, it also yielded similar results to prediction of Lorey's height from the largest trees using plots where all the trees were measured on the ground (supplementary figure 2b). This suggests that our conclusions are robust to the uncertainty introduced by height-diameter allometric models.

AGB prediction from the largest trees

429 We selected "20" as the number of largest trees to predict plot metrics. The resulting model

430 predicting AGB (Mg ha^{-1}) based on the 20 largest trees is:

431 $AGB = 0.0735 \times (Dg_{20}H_{20}WD_{20})^{1.1332}$ (rRMSE=0.179; R^2=0.85; AIC= -260.18) (10)

432 Because the exponent was close to 1, we also developed an alternative and more operationa

433 l model with the exponent constrained to 1, given by:

434 $AGB = 0.195 \times (Dg_{20}H_{20}WD_{20})$ (rRMSE=0.177; R^2=0.85; AIC=-195) (11)

435 Ground measurements of plot AGB were predicted by our N_{LT} model with the exponent

436 constrained to 1, with a total error of 17.9% (Figure 4), a value which encompass the error of

437 the N_{LT} model and the error related to the allometric model chosen. The Leave-One-Out cross-

438 validation procedure yielded similar results (rRMSE=0.19; R^2=0.81), validating the use of the

439 model on independent sites.

440 **Determining the cause of residual variations**

441 The explanatory variables all together explain about 37% of the variance in AGB both at plot

442 and site levels when omitting the diameter structure, and about 63% at site level when included

443 (Fig. 5). In general, forest structure and particularly the stem density explained most of the

444 residuals (table 1; weights: 79% and 54% at plot- and site-level respectively). The stem density

445 was followed by a continental effect (weights: 18%, 28% and 1%, respectively for Africa, South

446 America and Asia) and by the effect of H_{BA} and WD_{BA} (respective weights: 1% and 0% at the

447 plot level, 0% and 11% at the site level, and 23% and 0% when accounting for the diameter

448 structure at the site level). Inclusion of the diameter structure provided the best explanation of

449 residuals, with 63% of variance explained, and a weight of 69% for the first axis of the PCA

450 (supplementary figure 3). This first axis of the PCA was related to the general abundance of

451 trees at a site, and in particular medium-sized trees (40-60cm). Among environmental

452 variables, only rainfall was significantly related to the residuals at the site level when the

453 diameter structure was considered (2%).

Discussion

The largest trees, convergences and divergences between continents

Sampling a few largest trees per hectare generally allows an unbiased prediction of four key descriptors of forest structures across the Tropics. There is generally no improvement in predicting basal area, quadratic mean diameter, Lorey's height (H_{BA}) or community wood density beyond the first 10-to-20 largest trees (Figure 2, Figure 3a).In some cases, e.g. when a forest plot presents an abundant number of large trees (Figure 5d), increasing the number of trees sampled improves the model's accuracy. This is the case for BA for which rRMSE continues to decrease up to 100 largest trees (Figure 2a). In contrast, Lorey's height predictions are altered when a large number of trees are included (Figure 2c), i.e. when smaller, often suppressed, trees draw the average down (Farrior *et al.*, 2016). This might explain why the prediction of AGB does not mirror that of basal area (Figure 2b, Figure 3a), and suggest that the number of largest trees shall be set independently to each predictor considered. Interestingly, the evolution of relative error in AGB prediction as a function of the number of largest trees considered does not follow the same path between continents. For instance, the error of prediction saturates more quickly in Africa and Asia than Asia, where high variations of residuals are observed. Investigation of residuals showed that the diameter structure (Figure 5c, supplementary Figure 3b), and in particular the number of medium size trees (Figure 5d), drives variability in AGB predictions. It is therefore not surprising to see that in our dataset the site with higher levels of underestimations is the one with the highest number of medium size trees, which is found in Asia in the Western Ghats of India.

The good performance of models based on the 20 largest trees in predicting Lorey's height and community wood density at site level was not surprising. Both metrics were indeed weighted by basal area, driven *de facto* by the largest trees. Their consistency across sites and continents was not expected though. This suggests that the relationship between the 20 largest trees and descriptors of forest structures is stable across the tropics, and prove the generality of our approach. Slight differences are however noticeable when comparing the distribution of the pan-tropical model residuals across continents (Figure 6, supplementary

482 figure 4).In America, our pan-tropical model tend to slightly underestimate basal area (mean:

483 -5%) and overestimate Lorey's height (mean: +3%) (supplementary figure 4), suggesting

484 peculiar forest structures (i.e. higher tree height for a given diameter, and lower fractions of

485 large trees, supplementary figure 2). In Asia, and in particular in Africa, large (i.e. DBH > 50

486 cm) trees are more abundant and encompass a large fraction of plot biomass. The basal area

487 tends to be slightly overestimated in Africa, resulting in average to a 3% overestimation of AGB

488 (Figure 6a).

489 Interestingly, while a recent global phylogenetic classification of tropical forest groups

490 American with African forests vs. Asian forests (Slik *et al.*, 2018), our results tend more to

491 single out American forests. Although this deserves further investigations, it might reveal a lack

492 of close relationship between forest structure properties and phylogenic similarity, which

493 echoes recent results on the absence of relationship between tropical forest diversity and

494 biomass (Sullivan *et al.*, 2017).

495 **Largest trees, a gateway to global monitoring of tropical forests**

496 Revealing the predictive capacity held by the largest trees, our results constitute a major step

497 forward to monitor forest structures and biomass stocks. The largest trees in tropical forests

498 can therefore be used to accurately predict and efficiently infer various ground-measured

499 properties (i.e. the quadratic mean diameter, the basal area, Lorey's height and community

500 wood density), while previous work has predicted only biomass "estimates" (e.g. Slik *et al.*,

501 2013; Bastin *et al.*, 2015). This approach allows us to (i) describe forest structure independently

502 of any biomass allometric model (ii) and cover local variations in D-H relationship, known to

503 vary locally (Feldpausch *et al.*, 2011; Kearsley *et al.,* 2013;). It is also (iii) relatively insensitive

504 to differences in floristic composition and community wood density (Poorter *et al.*, 2015).

505 Furthermore, the "largest trees" models were developed for each plot-level metric and for any

506 number of largest trees. Thus, they do not rely on any arbitrary threshold of tree diameter. Note

507 that the optimal number of largest trees to be measured (i.e. 20) was set for demonstration

508 and can vary depending on the needs and capacities of each country or project (see

509 supplementary table 2). In the same way, local models could integrate locally-developed

510 biomass models, when available. Consequently our approach (i) can be used in young or

511 regenerating un-managed forests with a low "largest tree" diameter threshold and (ii) is

512 compatible with recent remote sensing approaches able to single out canopy trees and

513 describe their crown and height metrics (Ferraz *et al.*, 2016; Coomes *et al.*, 2017).

514 **Aboveground biomass model from the largest trees, a multiple opportunity**

515 Globally, the N_{LT} model for the 20 largest trees allows plot biomass to be predicted with 17.9%

516 error. This result is a pan-tropical validation of results obtained in Central Africa (Bastin *et al.*,

517 2015). It opens new perspectives towards cost-effective methods to monitor forest structures

518 and carbon stocks through largest trees metrics, i.e. metrics of objects directly intercepted by

519 remote-sensing products.

520 Developing countries willing to implement a Reduction of Emissions from Deforestation and

521 Forest Degradation (REDD+), shall also report on their carbon emissions (CE) and develop a

522 national CE reference level (IPCC, 2006; Maniatis & Mollicone, 2010). However, most tropical

523 countries lack capacities to assume multiple, exhaustive and costly forest carbon assessment

524 (Romijn *et al.*, 2012). By measuring only a few large trees per hectare, our results show that

525 it is possible to obtain unbiased estimates of aboveground C stocks in a time and cost-efficient

526 manner. Assuming that 400 to 600 trees D > 10 cm are measured in a typical 1-ha sample

527 plot, monitoring only 20 trees is a significant improvement. Although finding the 20 largest trees

528 in a plot of several hundred individuals requires evaluating more than 20 trees, in practice, a

529 conservative diameter threshold could be defined to ensure that the 20 largest trees are

530 sampled. An alternative approach could also be found in the development of relascope-based

531 approach adapted to detection of the largest trees in tropical forests. Using such approach

532 would facilitate rapid field sampling in extensive areas to produce large scale AGB estimates.

533 Those could fullfil the needs in calibration and validation of current and forthcoming space

534 missions focused on aboveground biomass.

535 Our findings also points towards the potential effectiveness of using remote sensing

536 techniques to characterize canopy trees. Here, remote sensing data could be used for direct

537 measurement (e.g. tree level metrics such as height, crown width, crown height) of the largest

538   trees instead of indirect development of complex metrics (e.g. mean canopy height, texture)

539   used to extrapolate forest properties. While some further refinements are needed, most of the

540   tools required to develop "largest trees" models are readily available. In particular, Ferraz et

541   al. (2016) developed an automated procedure to locate canopy trees based on airborne LiDAR

542   data, to measure their height and crown area. Crown area could further be linked to basal area,

543   as the logarithm of crown area is consistently correlated with a slope of 1.2-1.3 to the logarithm

544   of tree diameter across the tropics (Blanchard *et al.*, 2016). Regarding wood density,

545   hyperspectral signature offers a promising way to assess functional traits remotely (e.g. Asner

546   *et al.*, 2017) which could potentially be tested to detect variability in wood properties.

547   Alternative approaches could focus on the development of plot-level AGB prediction by

548   replacing the basal area of the largest trees with their crown metrics. While the measurement

549   of crown areas have yet to be generalized when inventorying plots, several biomass allometric

550   models already partition trunk and crown mass (Jucker *et al.*, 2016; Ploton *et al.*, 2016;

551   Coomes *et al.*, 2017).

552   The main limitation of our approach lies in the understory and sub-canopy trees. We show that

553   most of the remaining variance is explained by variations in diameter structures, and in

554   particular among the total stem density. Interestingly, stem density was generally identified as

555   a poor predictor of plot biomass in tropical forests (Slik *et al.*, 2010; Lewis *et al.*, 2013).

556   However, our results show that stem density explains most of the remaining variance (Table

557   S1). This suggests that, in addition to trying to understand large-scale variations in large trees

558   and other plot metrics, which can be directly quantified from remote sensing, we should also

559   put more effort into understanding variation in smaller trees, which mainly drives total stem

560   density and the total floristic diversity. Smaller trees are also essential to characterize forest

561   dynamics and understand changes in carbon stocks. Several options are nonetheless possible

562   from remote sensing, considering the variation in lidar point density below the canopy layer

563   (D'Oliveira *et al.*, 2012), the distribution of leaf area density (Stark *et al.*, 2012, 2015; Tang &

564   Dubayah, 2017) or the use of multitemporal lidar data to get information on forest gap

generation dynamics and consequently on forest diameter structure (Kellner *et al.*, 2009; Farrior *et al.*, 2016).

Large trees in degraded forests

If large trees are a key feature of unmanaged forests, they are conspicuously absent from managed or degraded forests. Indeed, large trees are targeted by selective or illegal logging, and are the first to disappear or to suffer from incidental damages when tropical forests are exploited for timber (Sist *et al.*, 2014). The loss of largest trees drastically changes forest structures and diameter distributions, and their loss is likely to counteract the consistency in forest structures observed through this study. Understanding how, or whether, managed forests deviate from our model predictions could help characterize forest degradation, which accounts for a large fraction of carbon loss worldwide (Baccini *et al.*, 2017), acknowledging that rapid post-disturbance biomass recovery (Rutishauser *et al.*, 2015) will remain hard to capture.

Conclusion – towards improved estimates of tropical forest biomass

The acquisition, accessibility and processing capabilities of very high spatial, spectral and temporal resolution remote sensing data has increases exponentially in recent years (Bastin *et al.*, 2017). However, to develop accurate global maps, we will have to obtain a greater number of field plots and develop new ways to use remote sensing data. Our results provide a step forward for both by (i) decreasing drastically the number of individual tree measurements required to get an accurate, yet less precise, estimate of plot biomass and (ii) opening the door to direct measurement of plot metrics measured from remote sensing to estimate plot biomass. As highlighted by Clark and Kellner (2012), new biomass allometric models relating plot-level biomass measured from destructive sampling and plot-level metric measured from remote-sensing products should be developed, as an alternative to current tree-level allometric models. Such an effort will lead largely to lower operational costs and uncertainties surrounding terrestrial C estimates, and consequently, will help developing countries in the development of national forest inventories and aid the scientific community in better understanding the effect of climate change on forest ecosystems.
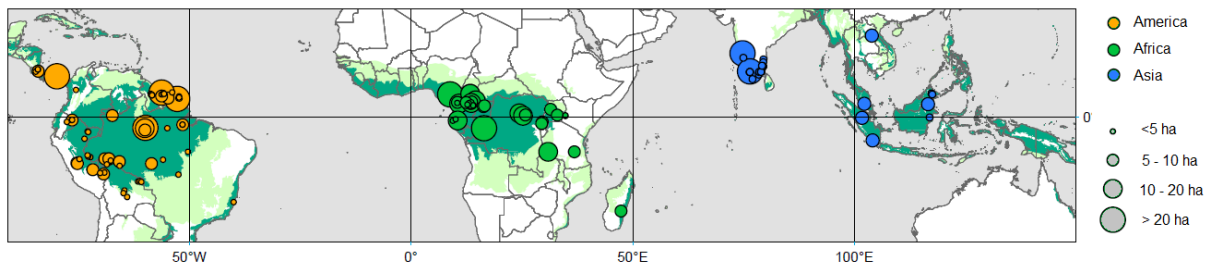
Contributions

J.F.Bastin and E.Rutishauser conceptualized the study, gathered the data, performed the analysis and wrote the manuscript. All the co-authors contributed by sharing data and reviewing the main text. A.R.Marshall, J.Poulsen and J.Kellner revised the English.

Conflict of interest

The authors declare there is no conflict of interest associated to this study.

Figures

Figure 1. Geographic distribution of the plot database. We used 867 plots of 1 hectare from 118 sites. Dots are colored according to floristic affinities (Slik et al. 2015), with America, Africa and Asia respectively in orange, green and blue. They are also sized according the total area surveyed in each site.

26
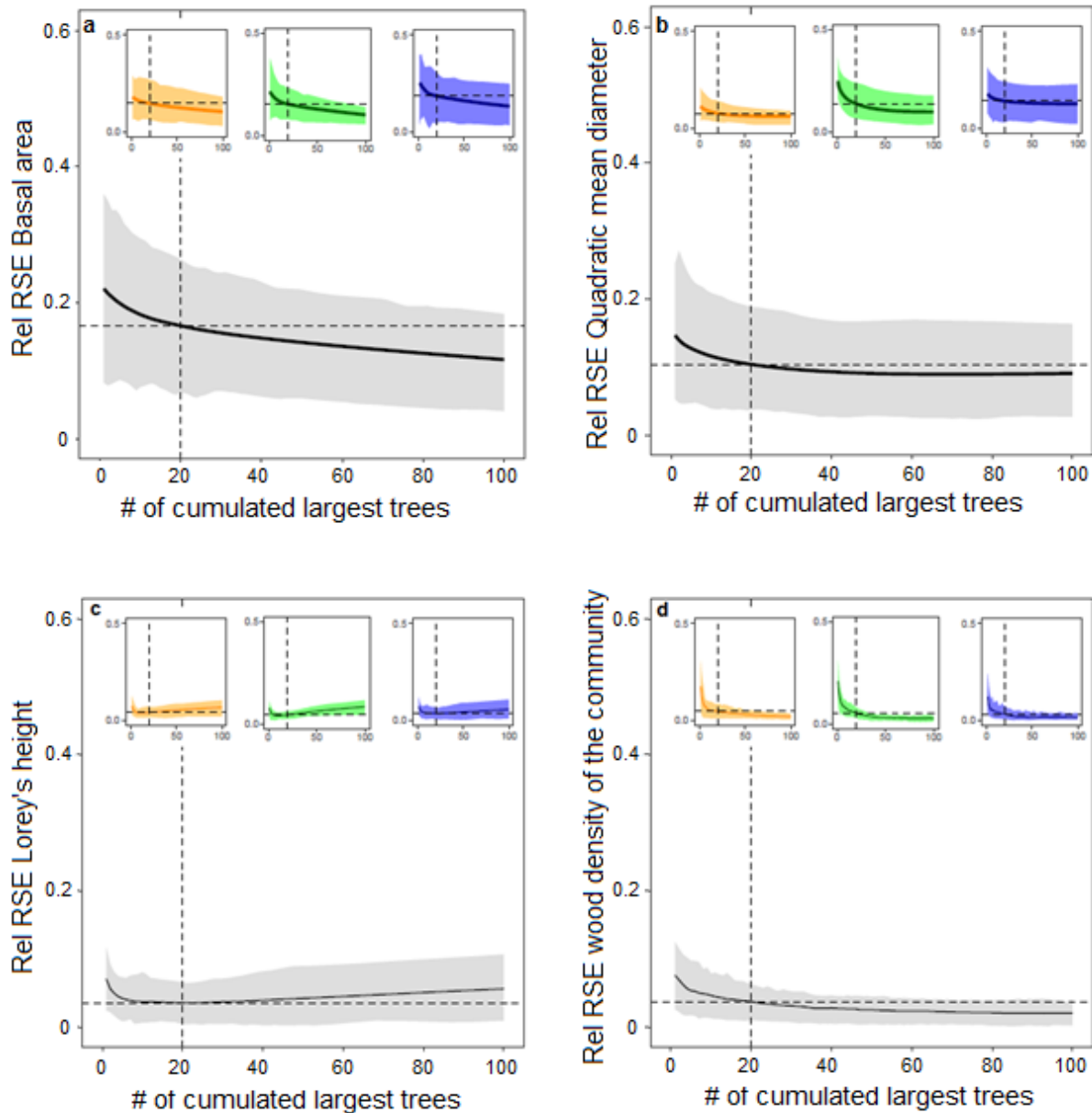
Figure 2. Quality of the prediction of plot metrics from largest trees. Variation of the relative Root Mean Square Error (rRMSE) of the prediction of plot metric from i largest trees versus the cumulative number of largest trees for (a) basal area, (b) quadratic mean diameter, (c) Lorey's height and (d) wood density weighted by the basal area. Results are displayed at the pan-tropical level (main plot in grey) and at the continental level (subplots; orange = America; green = Africa; blue = Asia). The solid line and shading shows the mean rRMSE and the 5th and the 95th percentiles. Dashed lines represent the mean rRMSE observed for each model, when considering the 20 largest trees.
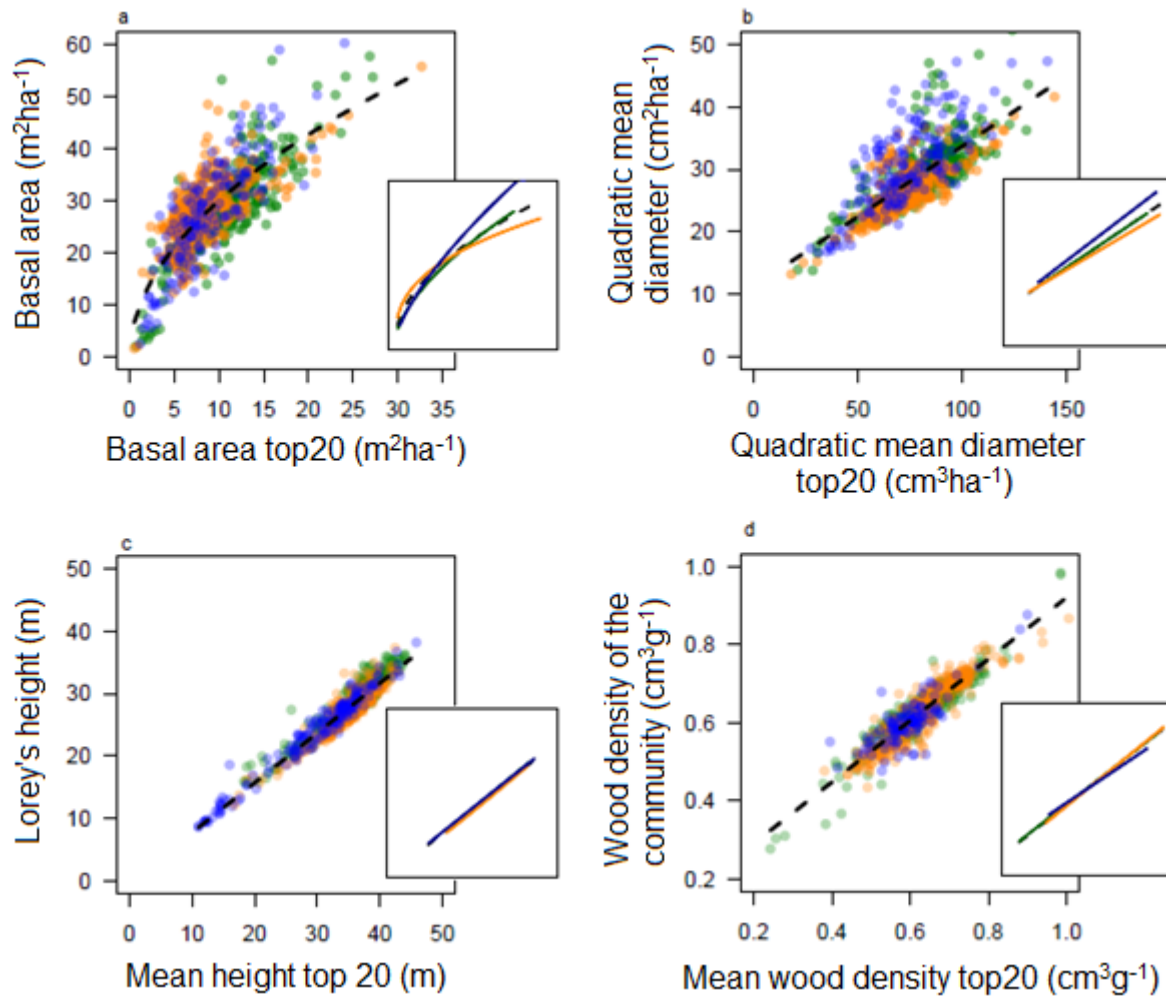
Figure 3. Prediction of plot metrics (y-axis) from the 20 largest trees (x-axis). Results are shown for (a) basal area, (b) quadratic mean diameter, (c) Lorey's Height and (d) wood density weighted by the basal area. Each dot corresponds to a single plot, colored in orange, green and blue for America, Africa and Asia respectively. Both pan-tropical (black dashed lines) and continental (coloured lines) regression models are displayed. These results show that substantial part of remaining variance, i.e. not explained by largest trees, is found when predicting the basal area and the quadratic mean diameter, with slight but significant differences between continents.
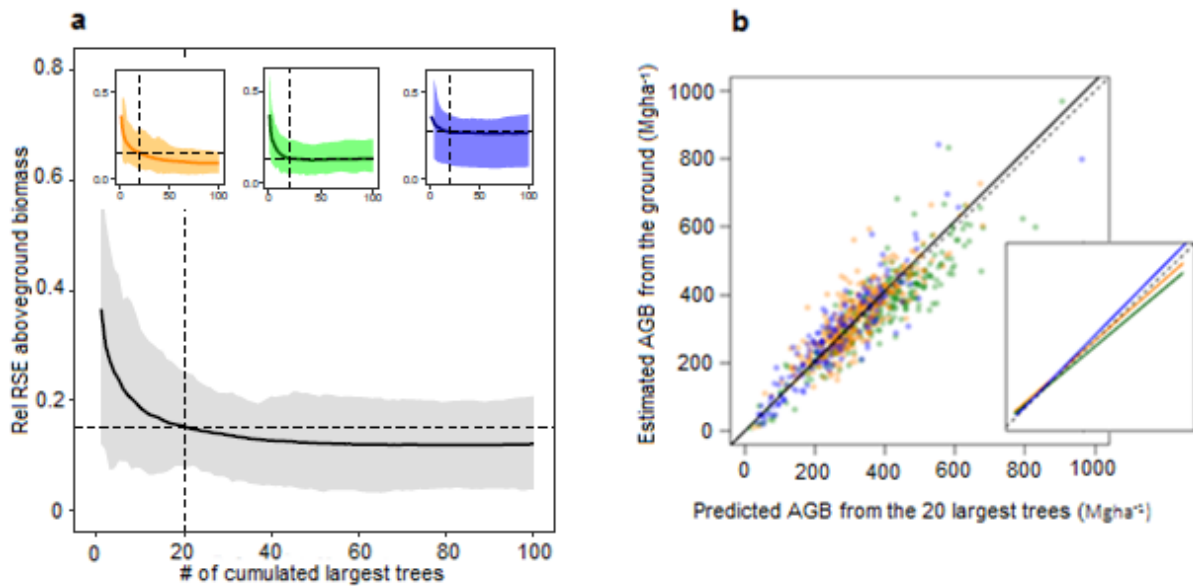
Figure 4. Prediction of AGB from plot metrics of the 20 largest trees. Results are shown for the 867 plots, among the three continents colored orange, green and blue for America, Africa and Asia respectively. The regression line of the model is shown as a continuous black line while the dashed black line shows a 1:1 relationship. The figure shows an unbiased prediction of AGB across the 867 plots, with slight but significant differences between the 3 continents.
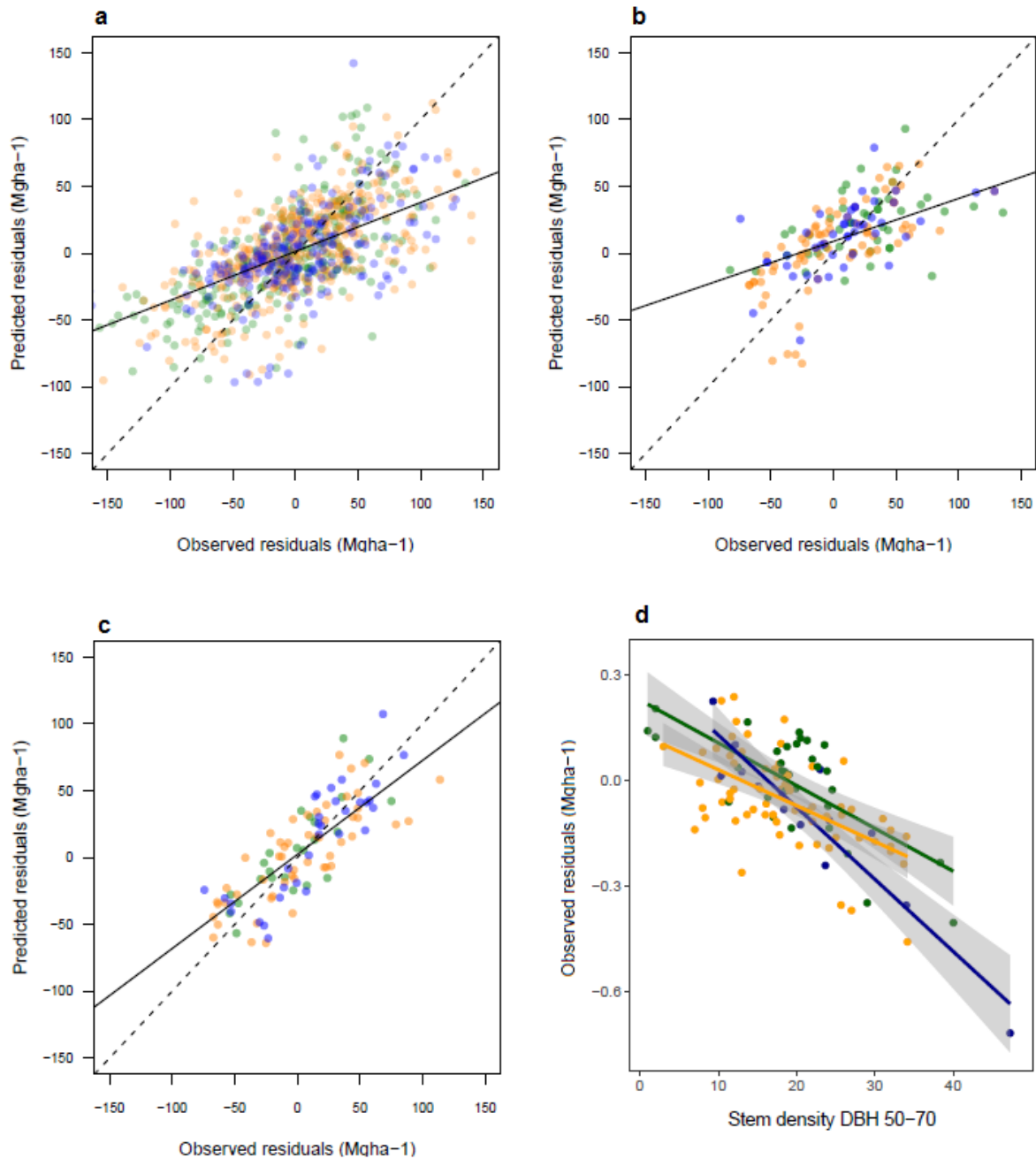
Figure 5. Predicted vs. observed residuals of above ground biomass predicted from the 20 largest trees. Residuals are explored at three different levels: (a) plot, (b) site [without considering the diameter structure as an explanatory variable], (c) site [considering the diameter structure] and (d) along the stem density of medium size trees. America, Africa and Asia are colored in orange, green and blue respectively. The figures show a good prediction of residuals in (a) and (b), driven by stem density, anda less biased prediction in (c), driven by

652   the diameter structure. Variance of observed residuals are also well explained by the stem

653   density of medium size trees (d), which mainly drive the first axis of the PCA.

654
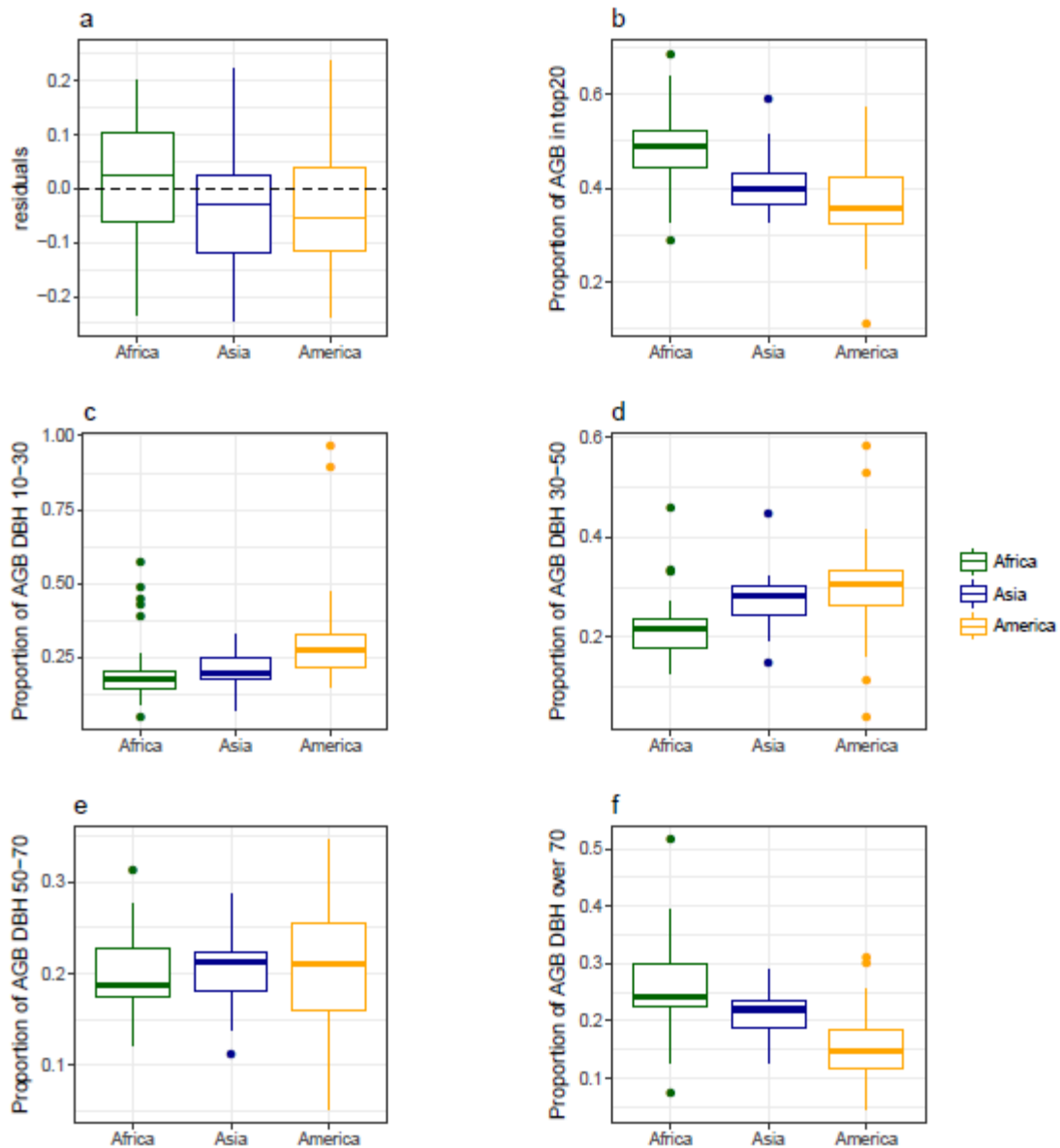
Figure 6. Comparison across continents of aboveground biomass prediction per site and their contribution to different share of the diameter structure. Africa, Asia and America, are colored in green, blue and orange, respectively. The distribution of the residuals of pan-tropical aboveground biomass prediction from the 20 largest trees (a) shows predictions are slightly overestimated in Africa (+2%), and slightly underestimated in Asia (-2%) and America (-6%). The proportion of aboveground biomass in the 20 largest trees (b) is highest in Africa (48%), followed by Asia (40%) and America (35%). The decomposition across four diameter classes (c-f, i.e. from 10 to 30, 30 to 50, 50 to 70 and beyond 70 cm) of their relative share of the total biomass shows that most of the biomass is found in the large trees in Africa, and in the small

664   to medium trees in America. Asia presenting a more balanced distribution of biomass across

665   the diameter structure.

Tables

Table 1. Weight of each variable retained for the explanation of AGB residuals. Weights are calculated as a type II sum of squares, which measures the decreased residual sum of squares due to an added variable once all the other variables have been introduced into the model. Results are shown for the exploration of residuals at the plot and at the site level, with and without consideration of the diameter structure. Weights are dominated by structural variables, and in particular the stem density and the diameter structure. Height, wood density and continent have also a non-negligible influence on residuals.

Level of residual	Parameter	Weight	674
Plot			
	Stem density*	79	
	Continent*	18	
	Lorey's height*	1	
	Major soil types	1	
	Temperature	1	
	Wood density weighted by the basal area	0	
	Rainfall	0	
Site without diametric structure			
	Stem density*	54	
	Continent*	28	
	Wood density weighted by the basal area*	11	
	Rainfall	3	
	Major soil types	3	
	Temperature	2	
	Lorey's height	0	
Site with diametric structure			
	PCA axis 1*	69	
	Lorey's height*	23	
	Rainfall*	3	
	Major soil types	3	
	Continent	1	
	Temperature	1	
	Wood density weighted by the basal area	0	
	PCA axis 2	0	

References

675 **References**

676 Asner, G.G.P., Mascaro, J., Muller-Landau, H.H.C., Vieilledent, G., Vaudry, R., Rasamoelina,

677   M., Hall, J.S. & van Breugel, M. (2012) A universal airborne LiDAR approach for tropical

678   forest carbon mapping. *Oecologia*, **168**, 1147–1160.

679 Asner, G.P., Martin, R.E., Knapp, D.E., Tupayachi, R., Anderson, C.B., Sinca, F., Vaughn,

680   N.R. & Llactayo, W. (2017) Airborne laser-guided imaging spectroscopy to map forest

681   trait diversity and guide conservation. *Science*, **355**.

682 Asner, G.P. & Mascaro, J. (2014) Mapping tropical forest carbon: Calibrating plot estimates

683   to a simple LiDAR metric. *Remote Sensing of Environment*, **140**, 614–624.

684 Baccini, A., Walker, W., Carvalho, L., Farina, M., Sulla-Menashe, D. & Houghton, R.A. (2017)

685   Tropical forests are a net carbon source based on aboveground measurements of gain

686   and loss. *Science (New York, N.Y.)*, **358**, 230–234.

687 Barbier, N. & Couteron, P. (2015) Attenuating the bidirectional texture variation of satellite

688   images of tropical forest canopies. *Remote Sensing of Environment*, **171**, 245–260.

689 Barbier, N., Proisy, C., Véga, C., Sabatier, D. & Couteron, P. (2011) Bidirectional texture

690   function of high resolution optical images of tropical forest: An approach using LiDAR

691   hillshade simulations. *Remote Sensing of Environment*, **115**, 167–179.

692 Bastin, J.-F., Barbier, N., Couteron, P., Adams, B., Shapiro, A., Bogaert, J., De Cannière, C.,

693   De Canniére, C. & De Cannière, C. (2014) Aboveground biomass mapping of African

694   forest mosaics using canopy texture analysis: toward a regional approach. *Ecological*

695   *Applications*, **24**, 1984–2001.

696 Bastin, J.-F., Barbier, N., Réjou-Méchain, M., Fayolle, A., Gourlet-Fleury, S., Maniatis, D., De

697   Haulleville, T., Baya, F., Beeckman, H., Beina, D., Couteron, P., Chuyong, G., Dauby,

698   G., Doucet, J.-L., Droissart, V., Dufrêne, M., Ewango, C., Gillet, J.F., Gonmadje, C.H.,

699   Hart, T., Kavali, T., Kenfack, D., Libalah, M., Malhi, Y., Makana, J.-R., Pélissier, R.,

700   Ploton, P., Serckx, A., Sonké, B., Stevart, T., Thomas, D.W., De Cannière, C. &

701   Bogaert, J. (2015) Seeing Central African forests through their largest trees. *Scientific*

702   *Reports*, **5**.

703 Bastin, J.-F., Berrahmouni, N., Grainger, A., Maniatis, D., Mollicone, D., Moore, R., Patriarca,

704   C., Picard, N., Sparrow, B., Abraham, E.M., Aloui, K., Atesoglu, A., Attore, F., Bassüllü,

705   Ç., Bey, A., Garzuglia, M., García-Montero, L.G., Groot, N., Guerin, G., Laestadius, L.,

706   Lowe, A.J., Mamane, B., Marchi, G., Patterson, P., Rezende, M., Ricci, S., Salcedo, I.,

707   Diaz, A.S.-P., Stolle, F., Surappaeva, V. & Castro, R. (2017) The extent of forest in

708   dryland biomes. *Science*, **356**, 635–638.

709 Bennett, A.C., McDowell, N.G., Allen, C.D. & Anderson-Teixeira, K.J. (2015) Larger trees

710   suffer most during drought in forests worldwide. *Nature Plants*.

711 Blanchard, E., Birnbaum, P., Ibanez, T., Boutreux, T., Antin, C., Ploton, P., Vincent, G.,

712   Pouteau, R., Vandrot, H., Hequet, V., Barbier, N., Droissart, V., Sonké, B., Texier, N.,

713   Kamdem, N.G., Zebaze, D., Libalah, M. & Couteron, P. (2016) Contrasted allometries

714   between stem diameter, crown area, and tree height in five tropical biogeographic

715   areas. *Trees*, **30**, 1953–1968.

716 Carré., F., Hiederer, R., Blujdea, V. & Koeble, R. (2010) *Background Guide for the*

717   *Calculation of Land Carbon Stocks in the Biofuels Sustainability Scheme Drawing on*

718   *the 2006 IPCC Guidelines for National Greenhouse Gas Inventories. EUR 24573 EN.*,

719   Luxembourg.

720 Chave, J., Coomes, D., Jansen, S., Lewis, S.L., Swenson, N.G. & Zanne, A.E. (2009)

721   Towards a worldwide wood economics spectrum. *Ecology letters*, **12**, 351–66.

722 Chave, J., Réjou-Méchain, M., Búrquez, A., Chidumayo, E., Colgan, M.S., Delitti, W.B.C.,

723   Duque, A., Eid, T., Fearnside, P.M., Goodman, R.C., Henry, M., Martínez-Yrízar, A.,

724   Mugasha, W.A., Muller-Landau, H.C., Mencuccini, M., Nelson, B.W., Ngomanda, A.,

725   Nogueira, E.M., Ortiz-Malavassi, E., Pélissier, R., Ploton, P., Ryan, C.M., Saldarriaga,

726   J.G. & Vieilledent, G. (2014) Improved allometric models to estimate the aboveground

727   biomass of tropical trees. *Global change biology*, **20**, 3177–3190.

728 Chave, J., Riera, B., Dubois, M.-A. & Riéra, B. (2001) Estimation of biomass in a neotropical

729   forest of French Guiana : spatial and temporal variability. *Journal of Tropical Ecology*,

730   **17**, 79–96.

731 Clark, D.B. & Clark, D.A. (1996) Abundance, growth and mortality of very large trees in

732   neotropical lowland rain forest. *Forest Ecology and Management*, **80**, 235–244.

733 Clark, D.B. & Clark, D.A. (2000) Landscape-scale variation in forest structure and biomass in

734   a tropical rain forest. *Forest Ecology and Management*, **137**, 185–198.

735 Clark, D.B. & Kellner, J.R. (2012) Tropical forest biomass estimation and the fallacy of

736   misplaced concreteness. *Journal of Vegetation Science*, **23**, 1191–1196.

737 Coomes, D.A., Dalponte, M., Jucker, T., Asner, G.P., Banin, L.F., Burslem, D.F.R.P., Lewis,

738   S.L., Nilus, R., Phillips, O.L., Phua, M.-H. & Qie, L. (2017) Area-based vs tree-centric

739   approaches to mapping forest carbon in Southeast Asian forests from airborne laser

740   scanning data. *Remote Sensing of Environment*, **194**, 77–88.

741 D'Oliveira, M.V.N., Reutebuch, S.E., McGaughey, R.J. & Andersen, H.-E. (2012) Estimating

742   forest biomass and identifying low-intensity logging areas using airborne scanning lidar

743   in Antimary State Forest, Acre State, Western Brazilian Amazon. *Remote Sensing of*

744   *Environment*, **124**, 479–491.

745 Farrior, C.E., Bohlman, S.A., Hubbell, S. & Pacala, S.W. (2016) Dominance of the

746   suppressed: Power-law size structure in tropical forests. *Science*, **351**.

747 Fayolle, A., Loubota Panzou, G.J., Drouet, T., Swaine, M.D., Bauwens, S., Vleminckx, J.,

748   Biwole, A., Lejeune, P. & Doucet, J.-L. (2016) Taller trees, denser stands and greater

749   biomass in semi-deciduous than in evergreen lowland central African forests. *Forest*

750   *Ecology and Management*, **374**, 42–50.

751 Feldpausch, T.R., Banin, L., Phillips, O.L., Baker, T.R., Lewis, S.L., Quesada, C. a., Affum-

752   Baffoe, K., Arets, E.J.M.M., Berry, N.J., Bird, M., Brondizio, E.S., de Camargo, P.,

753   Chave, J., Djagbletey, G., Domingues, T.F., Drescher, M., Fearnside, P.M., França,

754   M.B., Fyllas, N.M., Lopez-Gonzalez, G., Hladik, a., Higuchi, N., Hunter, M.O., Iida, Y.,

755   Salim, K. a., Kassim, a. R., Keller, M., Kemp, J., King, D. a., Lovett, J.C., Marimon,

756   B.S., Marimon-Junior, B.H., Lenza, E., Marshall, a. R., Metcalfe, D.J., Mitchard, E.T. a.,

757   Moran, E.F., Nelson, B.W., Nilus, R., Nogueira, E.M., Palace, M., Patiño, S., Peh, K.S.-

758   H., Raventos, M.T., Reitsma, J.M., Saiz, G., Schrodt, F., Sonké, B., Taedoumg, H.E.,

759 Tan, S., White, L., Wöll, H. & Lloyd, J. (2011) Height-diameter allometry of tropical forest

760 trees. *Biogeosciences*, **8**, 1081–1106.

761 Feldpausch, T.R., Lloyd, J., Lewis, S.L., Brienen, R.J.W., Gloor, E., Monteagudo Mendoza,

762 a., Lopez-Gonzalez, G., Banin, L., Abu Salim, K., Affum-Baffoe, K., Alexiades, M.,

763 Almeida, S., Amaral, I., Andrade, a., Aragão, L.E.O.C., Araujo Murakami, a., Arets,

764 E.J.M.M., Arroyo, L., Baker, T.R., Bánki, O.S., Berry, N.J., Cardozo, N., Chave, J.,

765 Comiskey, J. a., Dávila, E. a., de Oliveira, a., DiFiore, a., Djagbletey, G., Domingues,

766 T.F., Erwin, T.L., Fearnside, P.M., França, M.B., Freitas, M. a., Higuchi, N., Iida, Y.,

767 Jiménez, E., Kassim, a. R., Killeen, T.J., Laurance, W.F., Lovett, J.C., Malhi, Y.,

768 Marimon, B.S., Marimon-Junior, B.H., Lenza, E., Marshall, a. R., Mendoza, C.,

769 Metcalfe, D.J., Mitchard, E.T. a., Nelson, B.W., Nilus, R., Nogueira, E.M., Parada, a.,

770 Peh, K.S.-H., Pena Cruz, a., Peñuela, M.C., Pitman, N.C. a., Prieto, a., Quesada, C.

771 a., Ramírez, F., Ramírez-Angulo, H., Reitsma, J.M., Rudas, a., Saiz, G., Salomão,

772 R.P., Schwarz, M., Silva, N., Silva-Espejo, J.E., Silveira, M., Sonké, B., Stropp, J.,

773 Taedoumg, H.E., Tan, S., ter Steege, H., Terborgh, J., Torello-Raventos, M., van der

774 Heijden, G.M.F., Vásquez, R., Vilanova, E., Vos, V., White, L., Wilcock, S., Woell, H. &

775 Phillips, O.L. (2012) Tree height integrated into pan-tropical forest biomass estimates.

776 *Biogeosciences Discussions*, **9**, 2567–2622.

777 Ferraz, A., Saatchi, S., Mallet, C. & Meyer, V. (2016) Lidar detection of individual tree size in

778 tropical forests. *Remote Sensing of Environment*, **183**, 318–333.

779 Gibbs, H.K., Brown, S., Niles, J.O. & Foley, J. a (2007) Monitoring and estimating tropical

780 forest carbon stocks: making REDD a reality. *Environmental Research Letters*, **2**, 1–13.

781 Harms, K.E., Wright, S.J., Calderón, O., Hernández, a & Herre, E. a (2000) Pervasive

782 density-dependent recruitment enhances seedling diversity in a tropical forest. *Nature*,

783 **404**, 493–5.

784 Ho Tong Minh, D., Le Toan, T., Rocca, F., Tebaldini, S., Villard, L., Réjou-Méchain, M.,

785 Phillips, O.L., Feldpausch, T.R., Dubois-Fernandez, P., Scipal, K. & Chave, J. (2016)

786 SAR tomography for the retrieval of forest biomass and height: Cross-validation at two

787   tropical forest sites in French Guiana. *Remote Sensing of Environment*, **175**, 138–147.

788 IPCC (2006) *2006 IPCC Guidelines for National Greenhouse Gas Inventories, Prepared by*

789   *the National Greenhouse Gas Inventories Programme*, IGES. (ed. by H.S. Eggleston),

790   L. Buendia), K. Miwa), T. Ngara), and K. Tanabe) Japan, Japan.

791 Jucker, T., Caspersen, J., Chave, J., Antin, C., Barbier, N., Bongers, F., Dalponte, M., van

792   Ewijk, K.Y., Forrester, D.I., Haeni, M., Higgins, S.I., Holdaway, R.J., Iida, Y., Lorimer, C.,

793   Marshall, P.L., Momo, S., Moncrieff, G.R., Ploton, P., Poorter, L., Rahman, K.A.,

794   Schlund, M., Sonké, B., Sterck, F.J., Trugman, A.T., Usoltsev, V.A., Vanderwel, M.C.,

795   Waldner, P., Wedeux, B.M.M., Wirth, C., Wöll, H., Woods, M., Xiang, W., Zimmermann,

796   N.E. & Coomes, D.A. (2016) Allometric equations for integrating remote sensing

797   imagery into forest monitoring programmes. *Global Change Biology*, n/a-n/a.

798 Kearsley, E., de Haulleville, T., Hufkens, K., Kidimbu, A., Toirambe, B., Baert, G., Huygens,

799   D., Kebede, Y., Defourny, P., Bogaert, J., Beeckman, H., Steppe, K., Boeckx, P. &

800   Verbeeck, H. (2013) Conventional tree height-diameter relationships significantly

801   overestimate aboveground carbon stocks in the Congo Basin. *Nature communications*.

802 Kellner, J.R., Clark, D.B. & Hubbell, S.P. (2009) Pervasive canopy dynamics produce short-

803   term stability in a tropical rain forest landscape. *Ecology Letters*, **12**, 155–164.

804 Kellner, J.R. & Hubbell, S.P. (2017) Adult mortality in a low-density tree population using

805   high-resolution remote sensing. *Ecology*, **98**, 1700–1709.

806 Langsrud, Ø. (2003) ANOVA for unbalanced data: Use Type II instead of Type III sums of

807   squares. *Statistics and Computing*, **13**, 163–167.

808 Laurance, W.F., Delamônica, P., Laurance, S.G., Vasconcelos, H.L. & Lovejoy, T.E. (2000)

809   Conservation: Rainforest fragmentation kills big trees. *Nature*, **404**, 836–836.

810 Lewis, S.L.L., Sonké, B., Sunderland, T., Begne, S.K.S.K., Lopez-Gonzalez, G., Heijden,

811   G.M.F. Van Der, Phillips, O.L.O.L., Affum-Baffoe, K., Baker, T.R.T.R., Banin, L., Bastin,

812   J.-F.J.-F., Beeckman, H., Boeckx, P., Bogaert, J., De Cannière, C., Chezeaux, V., Clark,

813   C.J.C.J., Collins, M., Djagbletey, G., Droissart, V., Doucet, J.-L.J.-L., Ewango,

814   C.E.N.C.E.N., Fauset, S., Feldpausch, T.R.R., Foli, E.G., Gillet, J.-F.J.-F., Hamilton,

815 A.C.A.C., Harris, D.J.D.J., Hart, T.B.T.B., de Haulleville, T., Hladik, A., Hufkens, K.,

816 Huygens, D., Jeanmart, P., Jeffery, K.J., Kamdem, M.-N.D., Kearlsey, E., Leal, M.E.E.,

817 Lloyd, J., Lovett, J.C.J.C., Makana, J.-R.J.-R., Malhi, Y., Marshall, A.R.R., Ojo, L., Peh,

818 K.S.-H.K.S.-H., Pickavance, G., Poulsen, J.R., Reitsma, M., Sheil, D., Simo, M., Steppe,

819 K., Taedoumg, H.E.E., Talbot, J., Taplin, J.J.R.D., Taylor, D., Thomas, S.C.S.C.,

820 Toirambe, B., Verbeeck, H., Vleminckx, J., White, L.J.T.J.T., Willcock, S., Woell, H.,

821 Zemagho, L., van der Heijden, G.M.F., Phillips, O.L.O.L., Affum-Baffoe, K., Baker,

822 T.R.T.R., Banin, L., Bastin, J.-F.J.-F., Beeckman, H., Boeckx, P., Bogaert, J., De

823 Cannière, C., Chezeaux, E., Clark, C.J.C.J., Collins, M., Djagbletey, G., Djuikouo,

824 M.N.K., Droissart, V., Doucet, J.-L.J.-L., Ewango, C.E.N.C.E.N., Fauset, S., Feldpausch,

825 T.R.R., Foli, E.G., Gillet, J.-F.J.-F., Hamilton, A.C.A.C., Harris, D.J.D.J., Hart, T.B.T.B.,

826 de Haulleville, T., Hladik, A., Hufkens, K., Huygens, D., Jeanmart, P., Jeffery, K.J.,

827 Kearsley, E., Leal, M.E.E., Lloyd, J., Lovett, J.C.J.C., Makana, J.-R.J.-R., Malhi, Y.,

828 Marshall, A.R.R., Ojo, L., Peh, K.S.-H.K.S.-H., Pickavance, G., Poulsen, J.R., Reitsma,

829 J.M., Sheil, D., Simo, M., Steppe, K., Taedoumg, H.E.E., Talbot, J., Taplin, J.J.R.D.,

830 Taylor, D., Thomas, S.C.S.C., Toirambe, B., Verbeeck, H., Vleminckx, J., White,

831 L.J.T.J.T., Willcock, S., Woell, H. & Zemagho, L. (2013) Above-ground biomass and

832 structure of 260 African tropical forests. *Philosophical transactions of the Royal Society*

833 *of London. Series B, Biological sciences*, **368**.

834 Lindenmayer, D.B., Laurance, W.F. & Franklin, J.F. (2012) Global decline in large old trees.

835 *Science*, **338**, 1305–1306.

836 Malhi, Y., Wood, D., Baker, T.R., Wright, J., Phillips, O.L., Cochrane, T., Meir, P., Chave, J.,

837 Almeida, S., Arroyo, L., Higuchi, N., Killeen, T.J., Laurance, S.G., Laurance, W.F.,

838 Lewis, S.L., Monteagudo, A., Neill, D. a., Vargas, P.N., Pitman, N.C. a., Quesada, C.A.,

839 Salomao, R., Silva, J.N.M., Lezama, A.T., Terborgh, J., Martinez, R.V. & Vinceti, B.

840 (2006) The regional variation of aboveground live biomass in old-growth Amazonian

841 forests. *Global Change Biology*, **12**, 1107–1138.

842 Maniatis, D. & Mollicone, D. (2010) Options for sampling and stratification for national forest

843 inventories to implement REDD+ under the UNFCCC. *Carbon balance and*

844 *management*, **5**, 9.

845 Mascaro, J., Detto, M., Asner, G.P. & Muller-Landau, H.C. (2011) Evaluating uncertainty in

846 mapping forest carbon with airborne LiDAR. *Remote Sensing of Environment*, **115**,

847 3770–3774.

848 Meakem, V., Tepley, A.J., Gonzalez-Akre, E.B., Herrmann, V., Muller-Landau, H.C., Wright,

849 S.J., Hubbell, S.P., Condit, R. & Anderson-Teixeira, K.J. (2017) Role of tree size in

850 moist tropical forest carbon cycling and water deficit responses. *New Phytologist*.

851 Molto, Q., Hérault, B., Boreux, J.-J., Daullet, M., Rousteau, A. & Rossi, V. (2014) Predicting

852 tree heights for biomass estimates in tropical forests – a test from French Guiana.

853 *Biogeosciences*, **11**, 3121–3130.

854 Nepstad, D.C., Tohver, I.M., Ray, D., Moutinho, P. & Cardinot, G. (2007) Mortality of large

855 trees and lianas following experimental drought in an Amazon forest. *Ecology*, **88**,

856 2259–69.

857 New, M., Hulme, M., Jones, P., New, M., Hulme, M. & Jones, P. (1999) Representing

858 Twentieth-Century Space–Time Climate Variability. Part I: Development of a 1961–90

859 Mean Monthly Terrestrial Climatology. *Journal of Climate*, **12**, 829–856.

860 New, M., Lister, D., Hulme, M. & Makin, I. (2002) A high-resolution data set of surface

861 climate over global land areas. *Climate Research*, **21**, 1–25.

862 Ploton, P., Barbier, N., Couteron, P., Antin, C.M., Ayyappan, N., Balachandran, N., Barathan,

863 N., Bastin, J.-F., Chuyong, G., Dauby, G., Droissart, V., Gastellu-Etchegorry, J.-P.,

864 Kamdem, N.G., Kenfack, D., Libalah, M., Mofack, G., Momo, S.T., Pargal, S., Petronelli,

865 P., Proisy, C., Réjou-Méchain, M., Sonké, B., Texier, N., Thomas, D., Verley, P.,

866 Zebaze Dongmo, D., Berger, U. & Pélissier, R. (2017) Toward a general tropical forest

867 biomass prediction model from very high resolution optical satellite images. *Remote*

868 *Sensing of Environment*, **200**.

869 Ploton, P., Barbier, N., Takoudjou Momo, S., Réjou-Méchain, M., Boyemba Bosela, F.,

870 Chuyong, G., Dauby, G., Droissart, V., Fayolle, A., Goodman, R.C., Henry, M.,

Kamdem, N.G., Mukirania, J.K., Kenfack, D., Libalah, M., Ngomanda, A., Rossi, V.,

Sonké, B., Texier, N., Thomas, D., Zebaze, D., Couteron, P., Berger, U. & Pélissier, R.

(2016) Closing a gap in tropical forest biomass estimation: taking crown mass variation

into account in pantropical allometries. *Biogeosciences*, **13**, 1571–1585.

Ploton, P., Pélissier, R. & Proisy, C. (2012) Assessing aboveground tropical forest biomass

using Google Earth canopy images. *Ecological Applications*, **22**, 993–1003.

Poorter, L., van der Sande, M.T., Thompson, J., Arets, E.J.M.M., Alarcón, A., Álvarez-

Sánchez, J., Ascarrunz, N., Balvanera, P., Barajas-Guzmán, G., Boit, A., Bongers, F.,

Carvalho, F.A., Casanoves, F., Cornejo-Tenorio, G., Costa, F.R.C., de Castilho, C. V.,

Duivenvoorden, J.F., Dutrieux, L.P., Enquist, B.J., Fernández-Méndez, F., Finegan, B.,

Gormley, L.H.L., Healey, J.R., Hoosbeek, M.R., Ibarra-Manríquez, G., Junqueira, A.B.,

Levis, C., Licona, J.C., Lisboa, L.S., Magnusson, W.E., Martínez-Ramos, M., Martínez-

Yrizar, A., Martorano, L.G., Maskell, L.C., Mazzei, L., Meave, J.A., Mora, F., Muñoz, R.,

Nytch, C., Pansonato, M.P., Parr, T.W., Paz, H., Pérez-García, E.A., Rentería, L.Y.,

Rodríguez-Velazquez, J., Rozendaal, D.M.A., Ruschel, A.R., Sakschewski, B., Salgado-

Negret, B., Schietti, J., Simões, M., Sinclair, F.L., Souza, P.F., Souza, F.C., Stropp, J.,

ter Steege, H., Swenson, N.G., Thonicke, K., Toledo, M., Uriarte, M., van der Hout, P.,

Walker, P., Zamora, N. & Peña-Claros, M. (2015) Diversity enhances carbon storage in

tropical forests. *Global Ecology and Biogeography*, **24**, 1314–1328.

Proisy, C., Couteron, P. & Fromard, F. (2007) Predicting and mapping mangrove biomass

from canopy grain analysis using Fourier-based textural ordination of IKONOS images.

Remote Sensing of Environment, **109**, 379–392.

Réjou-Méchain, M., Tanguy, A., Piponiot, C., Chave, J. & Hérault, B. (2017) biomass : an r

package for estimating above-ground biomass and its uncertainty in tropical forests.

Methods in Ecology and Evolution, **8**, 1163–1167.

Remm, J. & Lõhmus, A. (2011) Tree cavities in forests – The broad distribution pattern of a

keystone structure for biodiversity. *Forest Ecology and Management*, **262**, 579–585.

Romijn, E., Herold, M., Kooistra, L., Murdiyarso, D. & Verchot, L. (2012) Assessing

899   capacities of non-Annex I countries for national forest monitoring in the context of

900   REDD+. *Environmental Science & Policy*, **19**–**20**, 33–48.

901   Rutishauser, E., Hérault, B., Baraloto, C., Blanc, L., Descroix, L., Sotta, E.D., Ferreira, J.,

902   Kanashiro, M., Mazzei, L., d'Oliveira, M.V.N., de Oliveira, L.C., Peña-Claros, M., Putz,

903   F.E., Ruschel, A.R., Rodney, K., Roopsind, A., Shenkin, A., da Silva, K.E., de Souza,

904   C.R., Toledo, M., Vidal, E., West, T.A.P., Wortel, V. & Sist, P. (2015) Rapid tree carbon

905   stock recovery in managed Amazonian forests. *Current biology : CB*, **25**, R787-8.

906   Rutishauser, E., Wagner, F., Herault, B., Nicolini, E.-A. & Blanc, L. (2010) Contrasting above-

907   ground biomass balance in a Neotropical rain forest. *Journal of Vegetation Science*,

908   672–682.

909   Saatchi, S.S., Houghton, R. a., Dos Santos Alvalá, R.C., Soares, J. V. & Yu, Y. (2007)

910   Distribution of aboveground live biomass in the Amazon basin. *Global Change Biology*,

911   **13**, 816–837.

912   Sist, P., Mazzei, L., Blanc, L. & Rutishauser, E. (2014) Large trees as key elements of

913   carbon storage and dynamics after selective logging in the Eastern Amazon. *Forest

914   Ecology and Management*, **318**, 103–109.

915   Slik, J.W.F., Aiba, S.-I., Brearley, F.Q., Cannon, C.H., Forshed, O., Kitayama, K., Nagamasu,

916   H., Nilus, R., Payne, J., Paoli, G., Poulsen, A.D., Raes, N., Sheil, D., Sidiyasa, K.,

917   Suzuki, E. & Van Valkenburg, J.L.C.H. (2010) Environmental correlates of tree biomass,

918   basal area, wood specific gravity and stem density gradients in Borneo's tropical forests.

919   *Global Ecology and Biogeography*, **19**, 50–60.

920   Slik, J.W.F., Alvarez-loayza, P., Alves, L.F., Ashton, P., Balvanera, P., Bastian, M.L.,

921   Bellingham, P.J., Berg, E. Van Den, Bernacci, L., Conceição, P., Blanc, L., Böhning-

922   gaese, K., Boeckx, P., Boyle, B., Bradford, M., Brearley, F.Q., Hockemba, B.,

923   Bunyavejchewin, S., Matos, C.L., Castillo-santiago, M., Eduardo, L.M., Chai, S., Chen,

924   Y., Colwell, R.K., Robin, C.L., Clark, C., Clark, D.B., Deborah, A., Culmsee, H., Damas,

925   K., Dattaraja, H.S., Dauby, G., Davidar, P., Dewalt, S.J., Doucet, J., Duque, A., Durigan,

926   G., Eichhorn, K.A.O., Pedro, V., Eler, E., Ewango, C., Farwig, N., Feeley, K.J., Ferreira,

927   L., Field, R., Ary, T., Filho, D.O., Fletcher, C., Forshed, O., Fredriksson, G., Gillespie, T.,

928   Amarnath, G., Griffith, D.M., Grogan, J., Gunatilleke, N., Harris, D., Harrison, R., Hector,

929   A., Homeier, J., Imai, N., Itoh, A., Jansen, P.A., Joly, C.A., Jong, B.H.J. De,

930   Kartawinata, K., Kearsley, E., Kelly, D.L., Kenfack, D., Kitayama, K., Kooyman, R.,

931   Larney, E., Laurance, S., Laurance, W.F., Michael, J., Leao, I., Letcher, S.G., Lindsell,

932   J., Lu, X., Mansor, A., Marjokorpi, A., Martin, E.H., Meilby, H., Melo, F.P.L., Metcalfe,

933   D.J., Vincent, P., Metzger, J.P., Millet, J., Mohandass, D., Juan, C., Nagamasu, H.,

934   Nilus, R., Ochoa-gaona, S., Paudel, E., Permana, A., Maria, T.F., Rovero, F., Rozak,

935   A.H., Santos, B.A., Santos, F., Sarker, S.K., Satdichanh, M., Schmitt, C.B., Schöngart,

936   J., Tabarelli, M., Tang, J., Targhetta, N., Theilade, I., Thomas, D.W., Tchouto, P.,

937   Hurtado, J., Valkenburg, J.L.C.H. Van, Do, T. Van, Verbeeck, H., Adekunle, V., Vieira,

938   S.A., Alvarez-loayza, P., Alves, L.F., Berg, E. Van Den & Bernacci, L. (2015) An

939   estimate of the number of tropical tree species. *Proceedings of the National Academy of*

940   *Sciences*, **112**, E4628–E4629.

941 Slik, J.W.F., Franklin, J., Arroyo-Rodríguez, V., Field, R., Aguilar, S., Aguirre, N., Ahumada,

942   J., Aiba, S.-I., Alves, L.F., Anitha, K., Avella, A., Mora, F., Aymard, G.A.C., Báez, S.,

943   Balvanera, P., Bastian, M.L., Bastin, J.-F., Bellingham, P.J., Van Den Berg, E., Da

944   Conceição Bispo, P., Boeckx, P., Boehning-Gaese, K., Bongers, F., Boyle, B.,

945   Brambach, F., Brearley, F.Q., Brown, S., Chai, S.-L., Chazdon, R.L., Chen, S., Chhang,

946   P., Chuyong, G., Ewango, C., Coronado, I.M., Cristóbal-Azkarate, J., Culmsee, H.,

947   Damas, K., Dattaraja, H.S., Davidar, P., DeWalt, S.J., Dln, H., Drake, D.R., Duque, A.,

948   Durigan, G., Eichhorn, K., Eler, E.S., Enoki, T., Ensslin, A., Fandohan, A.B., Farwig, N.,

949   Feeley, K.J., Fischer, M., Forshed, O., Garcia, Q.S., Garkoti, S.C., Gillespie, T.W.,

950   Gillet, J.-F., Gonmadje, C., Granzow-De La Cerda, I., Griffith, D.M., Grogan, J.,

951   Hakeem, K.R., Harris, D.J., Harrison, R.D., Hector, A., Hemp, A., Homeier, J., Hussain,

952   M.S., Ibarra-Manríquez, G., Hanum, I.F., Imai, N., Jansen, P.A., Joly, C.A., Joseph, S.,

953   Kartawinata, K., Kearsley, E., Kelly, D.L., Kessler, M., Killeen, T.J., Kooyman, R.M.,

954   Laumonier, Y., Laurance, S.G., Laurance, W.F., Lawes, M.J., Letcher, S.G., Lindsell, J.,

Lovett, J., Lozada, J., Lu, X., Lykke, A.M., Bin Mahmud, K., Mahayani, N.P.D., Mansor, A., Marshall, A.R., Martin, E.H., Matos, D.C.L., Meave, J.A., Melo, F.P.L., Mendoza, Z.H.A., Metali, F., Medjibe, V.P., Metzger, J.P., Metzker, T., Mohandass, D., Munguía-Rosas, M.A., Muñoz, R., Nurtjahy, E., De Oliveira, E.L., Onrizal, Parolin, P., Parren, M., Parthasarathy, N., Paudel, E., Perez, R., Pérez-García, E.A., Pommer, U., Poorter, L., Qi, L., Piedade, M.T.F., Pinto, J.R.R., Poulsen, A.D., Poulsen, J.R., Powers, J.S., Prasad, R.C., Puyravaud, J.-P., Rangel, O., Reitsma, J., Rocha, D.S.B., Rolim, S., Rovero, F., Rozak, A., Ruokolainen, K., Rutishauser, E., Rutten, G., Mohd Said, M.N., Saiter, F.Z., Saner, P., Santos, B., Dos Santos, J.R., Sarker, S.K., Schmitt, C.B., Schoengart, J., Schulze, M., Sheil, D., Sist, P., Souza, A.F., Spironello, W.R., Sposito, T., Steinmetz, R., Stevart, T., Suganuma, M.S., Sukri, R., Sultana, A., Sukumar, R., Sunderland, T., Supriyadi, Suresh, H.S., Suzuki, E., Tabarelli, M., Tang, J., Tanner, E.V.J., Targhetta, N., Theilade, I., Thomas, D., Timberlake, J., De Morisson Valeriano, M., Van Valkenburg, J., Van Do, T., Van Sam, H., Vandermeer, J.H., Verbeeck, H., Vetaas, O.R., Adekunle, V., Vieira, S.A., Webb, C.O., Webb, E.L., Whitfeld, T., Wich, S., Williams, J., Wiser, S., Wittmann, F., Yang, X., Yao, C.Y.A., Yap, S.L., Zahawi, R.A., Zakaria, R. & Zang, R. (2018) Phylogenetic classification of the world's tropical forests. *Proceedings of the National Academy of Sciences of the United States of America*, **115**.

Slik, J.W.F., Paoli, G., McGuire, K., Amaral, I., Barroso, J., Bastian, M., Blanc, L., Bongers, F., Boundja, P., Clark, C., Collins, M., Dauby, G., Ding, Y., Doucet, J.-L., Eler, E., Ferreira, L., Forshed, O., Fredriksson, G., Gillet, J.-F., Harris, D., Leal, M., Laumonier, Y., Malhi, Y., Mansor, A., Martin, E., Miyamoto, K., Araujo-Murakami, A., Nagamasu, H., Nilus, R., Nurtjahya, E., Oliveira, Á., Onrizal, O., Parada-Gutierrez, A., Permana, A., Poorter, L., Poulsen, J., Ramirez-Angulo, H., Reitsma, J., Rovero, F., Rozak, A., Sheil, D., Silva-Espejo, J., Silveira, M., Spironelo, W., ter Steege, H., Stevart, T., Navarro-Aguilar, G.E., Sunderland, T., Suzuki, E., Tang, J., Theilade, I., van der Heijden, G., van Valkenburg, J., Van Do, T., Vilanova, E., Vos, V., Wich, S., Wöll, H., Yoneda, T., Zang, R., Zhang, M.-G. & Zweifel, N. (2013) Large trees drive forest aboveground biomass

983   variation in moist lowland forests across the tropics. *Global Ecology and Biogeography*,

984   **22**, 1261–1271.

985 Stark, S.C., Enquist, B.J., Saleska, S.R., Leitold, V., Schietti, J., Longo, M., Alves, L.F.,

986   Camargo, P.B. & Oliveira, R.C. (2015) Linking canopy leaf area and light environments

987   with tree size distributions to explain Amazon forest demography. *Ecology Letters*, **18**,

988   636–645.

989 Stark, S.C., Leitold, V., Wu, J.L., Hunter, M.O., de Castilho, C. V., Costa, F.R.C., Mcmahon,

990   S.M., Parker, G.G., Shimabukuro, M.T., Lefsky, M.A., Keller, M., Alves, L.F., Schietti, J.,

991   Shimabukuro, Y.E., Brand??o, D.O., Woodcock, T.K., Higuchi, N., de Camargo, P.B.,

992   de Oliveira, R.C. & Saleska, S.R. (2012) Amazon forest carbon dynamics predicted by

993   profiles of canopy leaf area and light environment. *Ecology Letters*, **15**, 1406–1414.

994 Stegen, J.C., Swenson, N.G., Enquist, B.J., White, E.P., Phillips, O.L., Jørgensen, P.M.,

995   Weiser, M.D., Monteagudo Mendoza, A. & Núñez Vargas, P. (2011) Variation in above-

996   ground forest biomass across broad climatic gradients. *Global Ecology and*

997   *Biogeography*, **20**, 744–754.

998 Sullivan, M.J.P., Talbot, J., Lewis, S.L., Phillips, O.L., Qie, L., Begne, S.K., Chave, J., Cuni-

999   Sanchez, A., Hubau, W., Lopez-Gonzalez, G., Miles, L., Monteagudo-Mendoza, A.,

1000   Sonké, B., Sunderland, T., Ter Steege, H., White, L.J.T., Affum-Baffoe, K., Aiba, S.-I.,

1001   De Almeida, E.C., De Oliveira, E.A., Alvarez-Loayza, P., Dávila, E.Á., Andrade, A.,

1002   Aragão, L.E.O.C., Ashton, P., Aymard, G.A., Baker, T.R., Balinga, M., Banin, L.F.,

1003   Baraloto, C., Bastin, J.-F., Berry, N., Bogaert, J., Bonal, D., Bongers, F., Brienen, R.,

1004   Camargo, J.L.C., Cerón, C., Moscoso, V.C., Chezeaux, E., Clark, C.J., Pacheco, Á.C.,

1005   Comiskey, J.A., Valverde, F.C., Coronado, E.N.H., Dargie, G., Davies, S.J., De

1006   Canniere, C., Djuikouo, M.N., Doucet, J.-L., Erwin, T.L., Espejo, J.S., Ewango, C.E.N.,

1007   Fauset, S., Feldpausch, T.R., Herrera, R., Gilpin, M., Gloor, E., Hall, J.S., Harris, D.J.,

1008   Hart, T.B., Kartawinata, K., Kho, L.K., Kitayama, K., Laurance, S.G.W., Laurance, W.F.,

1009   Leal, M.E., Lovejoy, T., Lovett, J.C., Lukasu, F.M., Makana, J.-R., Malhi, Y.,

1010   Maracahipes, L., Marimon, B.S., Junior, B.H.M., Marshall, A.R., Morandi, P.S., Mukendi,

J.T., Mukinzi, J., Nilus, R., Vargas, P.N., Camacho, N.C.P., Pardo, G., Peña-Claros, M.,
Pétronelli, P., Pickavance, G.C., Poulsen, A.D., Poulsen, J.R., Primack, R.B., Priyadi,
H., Quesada, C.A., Reitsma, J., Réjou-Méchain, M., Restrepo, Z., Rutishauser, E.,
Salim, K.A., Salomão, R.P., Samsoedin, I., Sheil, D., Sierra, R., Silveira, M., Slik,
J.W.F., Steel, L., Taedoumg, H., Tan, S., Terborgh, J.W., Thomas, S.C., Toledo, M.,
Umunay, P.M., Gamarra, L.V., Vieira, I.C.G., Vos, V.A., Wang, O., Willcock, S. &
Zemagho, L. (2017) Diversity and carbon storage across the tropical forest biome.
Scientific Reports, **7**.

Tang, H. & Dubayah, R. (2017) Light-driven growth in Amazon evergreen forests explained
by seasonal variations of vertical canopy structure. *Proceedings of the National
Academy of Sciences of the United States of America*, **114**, 2640–2644.

Thomas, R.Q., Kellner, J.R., Clark, D.B. & Peart, D.R. (2013) Low mortality in tall tropical
trees. *Ecology*, **94**, 920–929.

West, G.B., Enquist, B.J., Brown, J.H., West, G.B., Brown, J.H., Enquist, B.J. & Brown, J.H.
(2009) Extensions and evaluations of a general quantitative theory of forest structure
and dynamics. *Proceedings of the National Academy of Sciences of the United States
of America*, **106**, 7040–7045.

Zanne, A.E., Lopez-Gonzalez, G., Coomes, D.A., Ilic, J., Jansen, S., Lewis, S.L., Miller, R.B.,
Swenson, N.G., Wiemann, M.C. & Chave, J. (2009) Global wood density database.
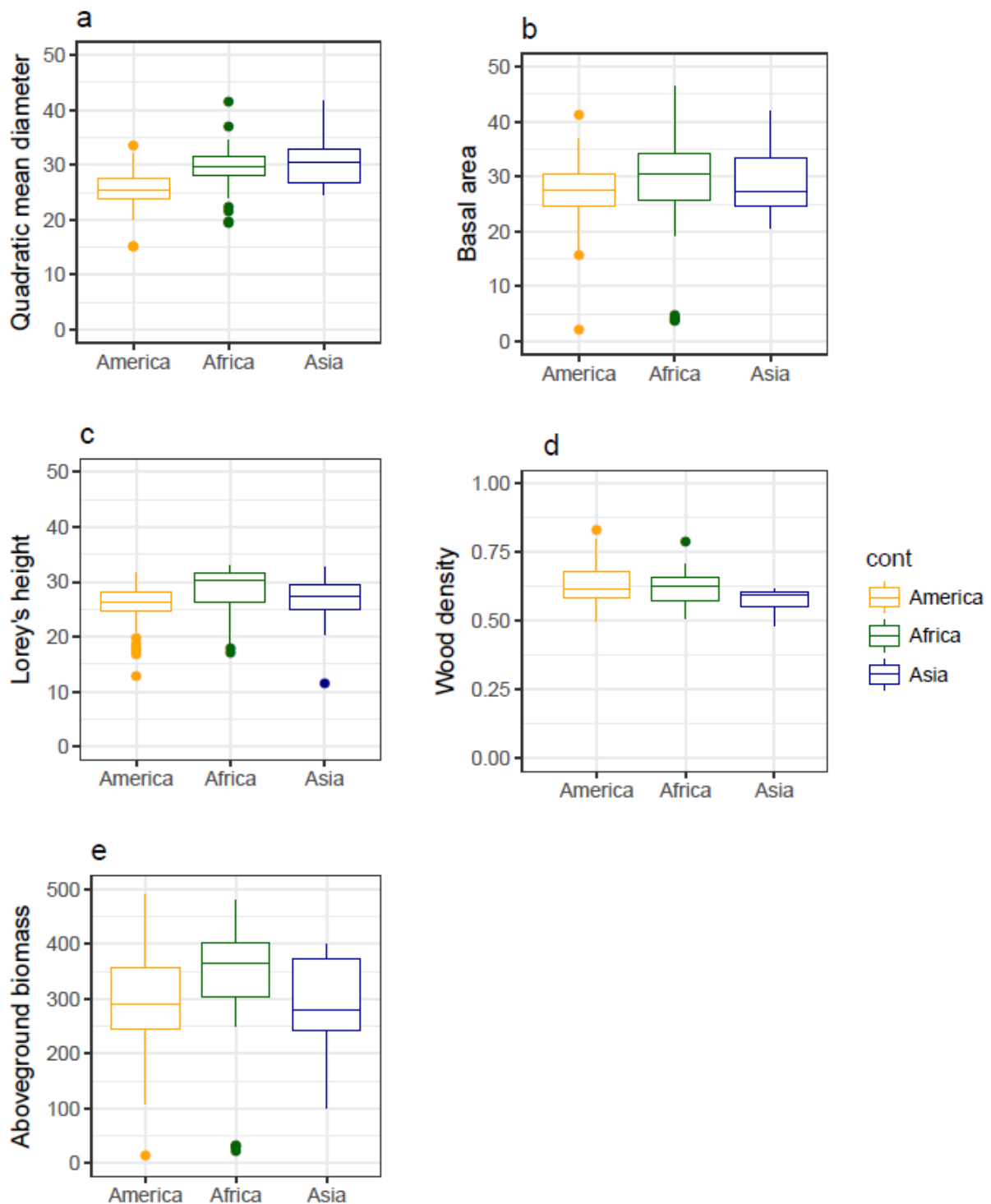*Dryad*, **235**, 33.

1032 **Supplementary information.**

1033 **Supplementary table 1. Plot, Site and PIs**

1034 **Supplementary table 2. Coefficients of plot level structure prediction from the *ith***
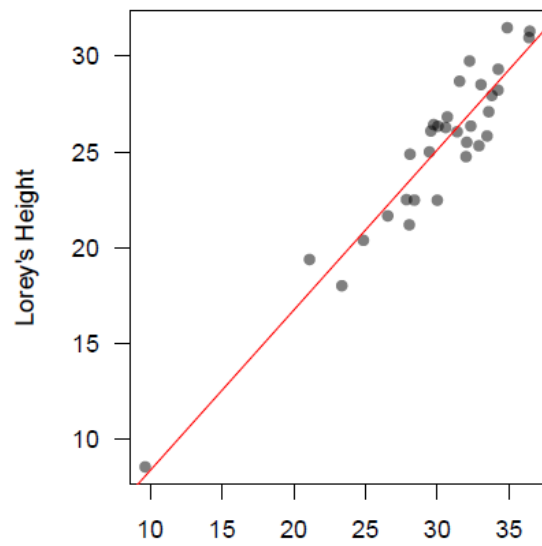
1035 **largest trees.**

Supplementary figure 1. Cross-continent comparison of plot-metrics distribution averaged at the site level. Figures illustrates respectively the distribution of the values for the quadratic mean diameter (a), basal area (b), Lorey's height (c), wood density (d) and aboveground biomass (e).
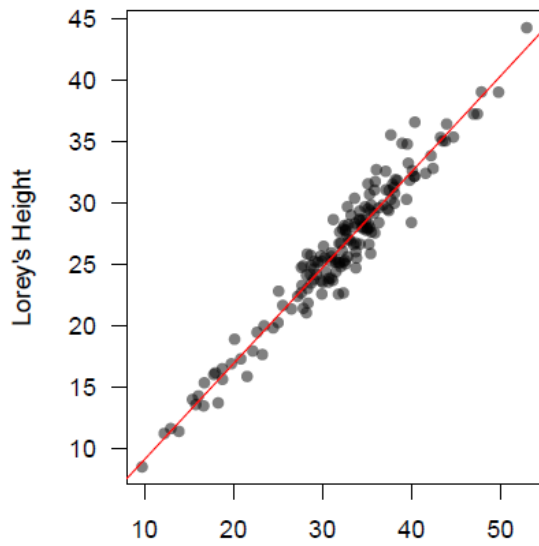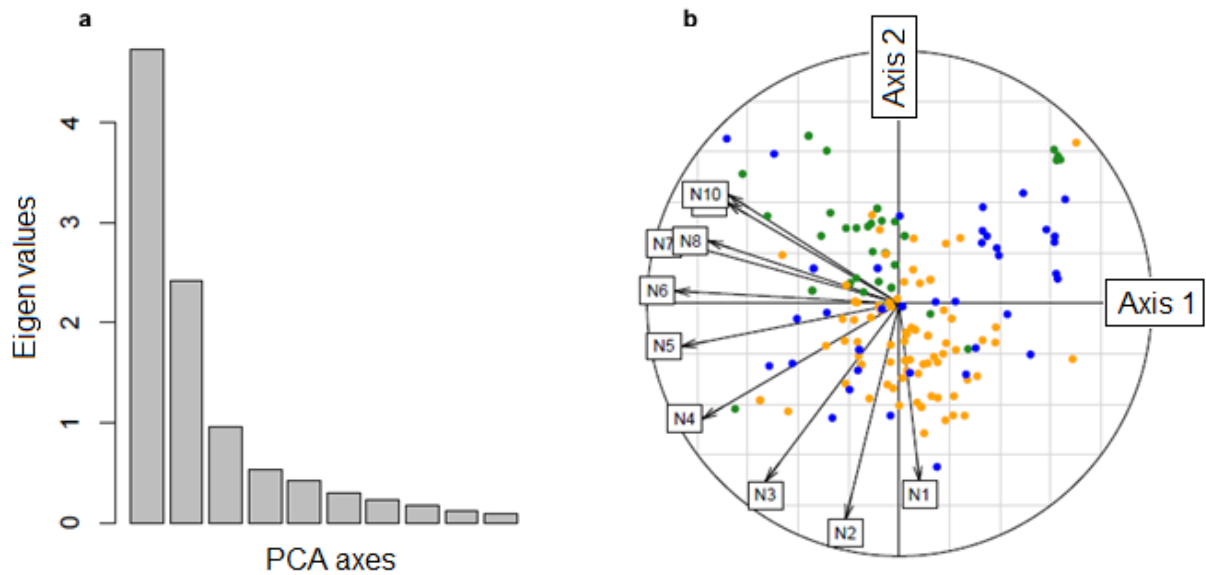
Supplementary figure 2. Lorey's Height prediction from the 20 largest trees. Figures

show the results using (i) local D-H allometries for 20 sites (left subfigure) and (ii) using plots

where height is measured on all trees in Malebo site in the Democratic Republic of the Congo

(right subfigure).

Supplementary figure 3. PCA on the diameter structure and corresponding mean distribution for high contributions of axis 1 and axis 2. (A) Illustration of top and low percentile observed for each axis, with diameter distributions represented as the relative difference with the average observed distribution.(B) Biplot with contribution to the PCA of all the diameter classes, with the respective position of each site in the space defined by axis1 and 2. Axis 1 is driven by differences in global abundance of trees and axis 2 is driven by a difference of balance between abundance of small vs. large trees. Colors represent continent, with Africa, America and Asia respectively in green, orange and blue.
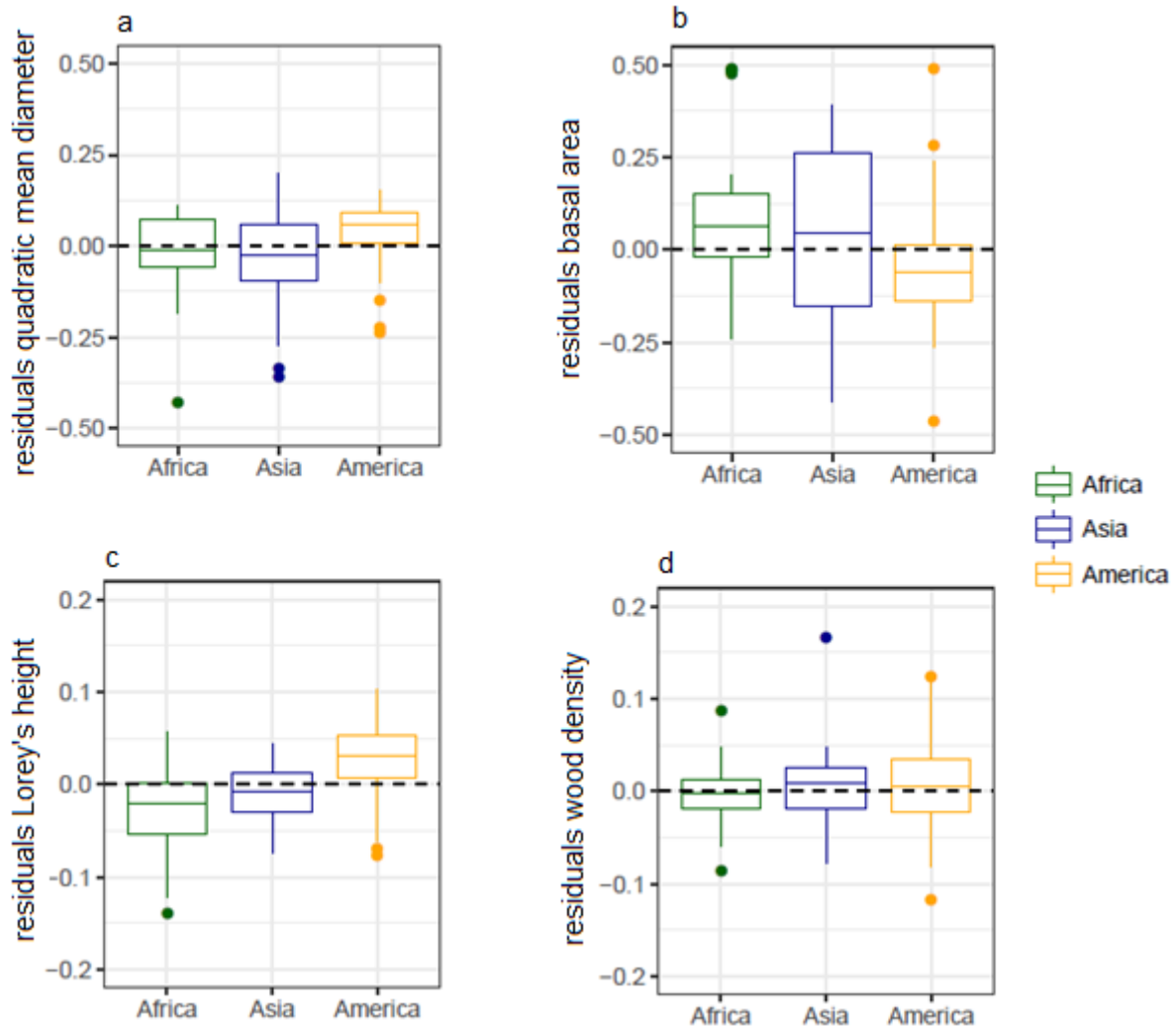
Supplementary figure 4. Cross-continent comparison of the relative residuals from the prediction of plot-metrics from the 20 largest trees. The relative residuals are generally low (<10%). Systematic small differences can however be found in America, where the quadratic mean diameter and Lorey's height tend to be slightly overestimated and the basal area slightly underestimated.